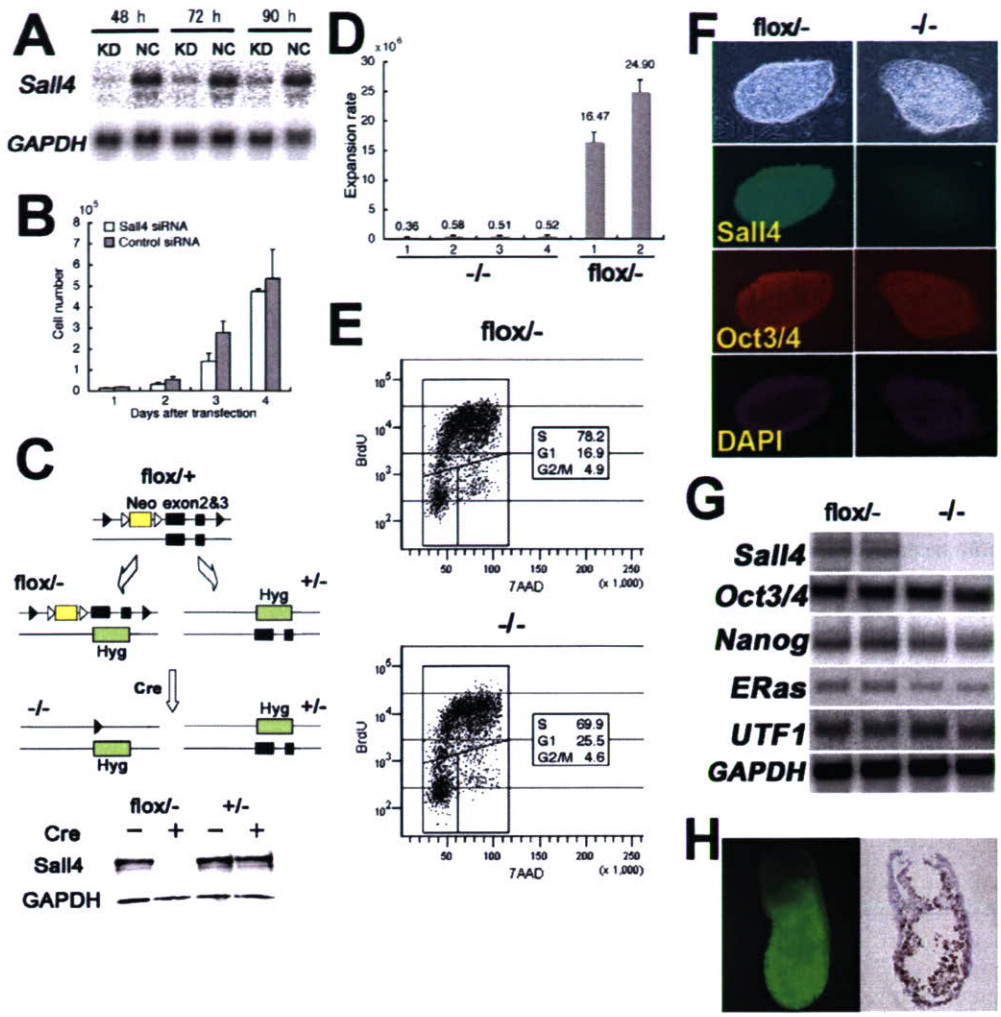

Fig. 3. Reduced proliferation of *Sall4*-null ES cells. (**A**) Northern blot analysis showing the reduction of *Sall4* upon Sall4-siRNA treatment. KD (knockdown), treated with Sall4-siRNA; NC (negative control), treated with control siRNA. (**B**) Transiently reduced proliferation of ES cells upon Sall4-siRNA treatment. Cells were counted in triplicate. (**C**) Conditional disruption of *Sall4* in ES cells. When a *Sall4-IRES-Hyg* vector was introduced into cells heterozygous for a floxed allele of *Sall4* (flox/+), both alleles were targeted with a similar frequency, resulting in two types of cells: flox/– and +/–. Upon infection with adenovirus expressing Cre, flox/– cells became almost *Sall4*-null by day 3, determined by western blot (lowest panels). White triangle, Frt; black triangle, loxP. (**D**) Reduced proliferation of *Sall4*-null ES cells. Cell expansion rate over 16 days is shown, using *Sall4*-null (–/–) versus flox/– cells obtained upon the same Cre treatment. Analysis was carried out in triplicate. (**E**) Reduced S phase and increased G1 phase in the *Sall4*-null ES cells. Consistent data were obtained from two independent experiments using three *Sall4*-null cells, and the representative data is shown. (**F**) Normal morphology and positive staining of Oct3/4 of a *Sall4*-null ES colony. (**G**) Northern blot analysis of *Sall4*-deficient ES cells. Two heterozygous (flox/–), and two *Sall4*-null ES (–/–) clones are shown. (**H**) Chimeric embryo formation from *Sall4*-null ES cells transfected with GFP. (left) High contribution of GFP-expressing cells in the E7.5 embryo. (Right) A section of the chimera was stained by an anti-GFP antibody and detected by DAB.

were picked, 44 out of 47 clones were *Sall4* null, and all these *Sall4*-null clones grew significantly slower than the clones retaining *Sall4* despite being treated identically (Fig. 3D), but could be cultured for a prolonged period of time (more than 1 month). None of the clones from the other groups (flox/– without Cre, +/– with or without Cre) showed impaired proliferation, and re-expression of *Sall4* cDNA under a ubiquitous promoter in *Sall4*-null cells restored proliferation (data not shown), confirming that this phenotype was *Sall4* dependent. Cell cycle analysis revealed that *Sall4*-null cells showed a decreased S-phase and increased G1-phase compared with heterozygous cells (Fig. 3E). These data suggest that *Sall4* absence in ES cells leads to inefficient G1/S transition, which may possibly explain the phenotypes observed in blastocyst culture and embryos in vivo.

These *Sall4*-null ES cells formed compact colonies and were morphologically indistinguishable from heterozygous or wild-type cells (Fig. 3F). No significant differences were observed in LIF-induced STAT3 phosphorylation or BMP4-induced Id family upregulation between wild-type and *Sall4*-null ES cells, suggesting that the absence of *Sall4* does not affect the response to the two major extrinsic signals involved in maintaining the pluripotency of ES cells (data not shown). In the *Sall4*-null ES cells, *Oct3/4* and *Nanog*, which are essential for pluripotency, and *Eras* and *Utf1*, which are important for the growth properties of the ES cells, continued to be expressed, which was confirmed by northern blot and immunostaining (Fig. 3F,G). Although expression of *Oct3/4* and *Utf1* was unaltered in the absence of *Sall4*, the expression of *Nanog* and *Eras* was slightly decreased, and this was detailed in the discussion. Expression of markers for primitive endoderm (*Gata6*), mesoderm (*T*), and trophectoderm (*Cdx2*) was not detected (data not shown), which suggests that the proliferation defect observed in the absence of Sall4 is not secondary to aberrant differentiation. Embryoid bodies were formed, though were smaller, from *Sall4*-null ES cells, and *Sall4*-deficient cells produced markedly smaller tumors than did heterozygous cells when transplanted into nude mice (data not shown), again suggesting that *Sall4* absence does not affect pluripotency of ES cells but proliferation. To further confirm that *Sall4*-null cells are undifferentiated, we injected these cells into

Table 3. Increased death rate of *Sall4* heterozygous mice after birth

Age	+/+	+/–
0-3 weeks	1	13
3-6 weeks	0	8
Total: dead/born (%)	1/80 (1.3)	21/86 (24.4)

Dead pups from the heterozygous crosses (described in Table 1) were scored for 6 weeks after birth.

blastocysts to generate chimeras. At E7.5, *Sall4*-null cells tagged with GFP contributed highly to the embryos (Fig. 3H). Taken together, our data indicate that Sall4 is essential for proliferation but not pluripotency of ES cells.

Sall4 haploinsufficiency results in anorectal and heart anomalies and exencephaly

Genotyping from heterozygous crosses showed that nearly half the *Sall4* heterozygous mice died in utero (Table 1). Out of 86 born heterozygous mice, 13 were runt and died or were eaten by their mothers within 3 weeks (Table 3). Eight more died within the next 3 weeks and six of these mice had significantly dilated bowels and apparent anal stenosis (Fig. 4A, open arrowhead). The number of enteric ganglia in these heterozygotes was not affected (data not shown); hence, gastrointestinal dilation is likely to be a secondary effect of anal dysplasia. When examined at E17.5-18.5, ventricular septum defects were also observed in some of the heterozygotes (Fig. 4B and Table 4). These phenotypes partially mimic the Okihiro syndrome caused by *SALL4* mutations in humans, and, thus, anorectal and heart anomalies could be caused by *SALL4* haploinsufficiency. Other phenotypes observed in Okihiro syndrome were not detected in *Sall4*-heterozygous mice. All the heterozygotes that survived beyond 3 weeks (n=73) had normal appearing extremities and closer examination of newborns did not show any anomalies in digit, metacarpus or metatarsus formation (n=6) (Fig. 4C). Though abducens nerves and nuclei are reported to be responsible for the abnormal eye movements in Okihiro syndrome (Al-Baradie et al., 2002; Kohlhase et al., 2002), the abducens nuclei in adult heterozygous mice (n=6) were properly formed, and oculomotor and trochlear nuclei, eye and ocular muscles were also unaffected (Fig. 4D and data not shown). Inner ear structures at E17.5 (n=9) and in adults (n=6) were not impaired (Fig. 4E; data not shown). Thus, in mice, not all Okihiro phenotypes were caused by Sall4 haploinsufficiency.

We also found other phenotypes not reported in humans. Some heterozygotes (three out of 26 examined at E11.5-15.5) exhibited exencephaly (Fig. 4F), and four out of 73 *Sall4* heterozygous mice that survived up to 3 weeks exhibited tail flexion anomalies (data not shown). As exencephaly and a kinked tail are caused by failure of the neural tube to close, *Sall4* may also play an important role in this event.

Sall4 genetically interacts with *Sall1*

Compound heterozygotes were generated to investigate functional redundancy among members of the *Sall* family. Surprisingly, no *Sall1/4* compound heterozygotes survived after birth, whereas mice having other genetic combinations (*Sall1/2*, *Sall1/3*, *Sall2/3*, *Sall2/4* and *Sall3/4*) survived. The *Sall1/4* heterozygotes exhibited uni- or bilateral renal agenesis (Fig. 5A), exencephaly (data not shown), anorectal malformations (Fig. 5B) and ventricular septum defects (data not shown); the incidence of these phenotypes was significantly increased in comparison with *Sall4* heterozygotes (Table 4), suggesting a genetic interaction of *Sall4* and *Sall1* in vivo. Next, we determined if the expression of *Sall4* and *Sall1* overlapped in the affected organs. At E8.5, a stage at which the neural tubes close, both *Sall4* and *Sall1* were expressed in the mesenchyme of the anterior portion (Fig. 5C, filled arrowhead) and in all tissues of the tail region (Fig. 5C, open arrowhead). At E11.5, *Sall4* and *Sall1* were expressed in the anorectal region (Fig. 5D, arrowhead). In the heart at E11.5, *Sall4* was detected in the myocardium, including the developing interventricular septum, while *Sall1* was expressed not only in the myocardium but also in the endocardium, thus overlapping with *Sall4* in the myocardium (Fig. 5E). We further checked to determine if Sall1 and Sall4 were colocalized in ES cells. Endogenous Sall4 was localized in the punctate nuclear foci that colocalized with 4,6-diamidino-2-phenylindole (DAPI) (Fig. 5F), indicating that Sall4 is localized in the constitutive heterochromatin. Endogenous Sall1 was also localized in the heterochromatin and overlapped with Sall4. Immunoprecipitation using lysates from ES cells showed that endogenous Sall4 binds to Sall1 (Fig. 5G). Therefore, these two genes probably form heterodimers in the developing brain, heart and anorectal regions.

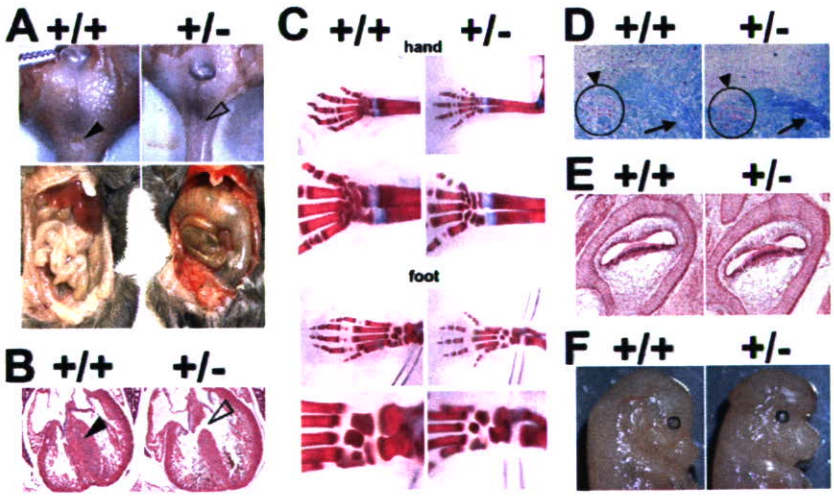

Fig. 4. Phenotypes caused by *Sall4* haploinsufficiency. (**A**) Anal stenosis (above) and megacolon (below) of 5-week-old *Sall4*-heterozygous mice. Black arrowhead, anus in wild type; open arrowhead, imperforate anus in the heterozygotes. (**B**) Ventricular septum defect in *Sall4* heterozygotes at E18.5. Black arrowhead, ventricular septum in wild-type; open arrowhead, ventricular septum defect in the heterozygotes. Hematoxylin and Eosin staining. (**C**) Normal formation of digits, metacarpus and metatarsus in new born *Sall4* heterozygotes. Stained with Alcian Blue and Alizarin Red S. (**D**) Normal formation of abducens nuclei (arrowhead) and facial nerve (arrow) in 8-week-old *Sall4* heterozygotes. Serial sections were examined by Klüver-Barrera staining. (**E**) Normal development of inner ear structure in *Sall4* heterozygotes at E17.5. Hematoxylin and Eosin staining. (**F**) Exencephaly of *Sall4*-heterozygous mice at E14.5.

Table 4. Phenotypic exacerbation in *Sall4/Sall1* double heterozygous mice

	Sall4+/–	*Sall1+/–*	*Sall4+/– Sall1+/–*
Renal agenesis*	0/43 (0%)	2/61 (3.3%)‡	16/38 (42.1%)§
Exencephaly*	2/43 (4.6%)	0/61 (0%)	17/38 (44.7%)
Anorectal malformations†	4/14 (28.6%)	0/14 (0%)	11/16 (68.8%)
Ventricular septum defects†	2/10 (20.0%)	0/10 (0%)	7/10 (70.0%)

*Examined at E13.5-P0.
†Examined at E17.5-18.5.
‡Two *Sall1* heterozygotes had unilateral kidney agenesis.
§Six out of 16 double heterozygotes had no kidneys bilaterally, and ten had unilateral kidney agenesis.

However, in the developing kidney, the two genes did not overlap (data not shown). Thus, heterodimer-independent mechanisms may exist in kidney development.

Truncated Sall1 disturbs heterochromatin localization of Sall4, and functions in a dominant-negative manner

When various *Sall4* and *Sall1* constructs with mutations in the zinc-finger domains were generated, we observed that the most C-terminal double zinc-finger domain (Zn4) of Sall4 was essential and sufficient for localization to the heterochromatin (Fig. 6A). In the case of Sall1, two double zinc fingers (Zn 4 and 5) were required, and were sufficient for heterochromatin localization (Fig. 6B). Thus, these C-terminal double zinc fingers constitute heterochromatin localization domains. *SALL1* mutations in Townes-Brocks syndrome are likely to produce C-terminally truncated proteins. Truncated *Sall1* fused to *DsRed* (*Sall1*$^{1\text{-}435}$*-DsRed*) was ubiquitously located throughout the cytoplasm and euchromatin (Fig. 6C), as this mutant lacked the C-terminal heterochromatin localization domain. Co-transfection of *Sall1*$^{1\text{-}435}$*-DsRed* and *Sall4-GFP* showed disturbance in Sall4 localization in the heterochromatin. Thus, the C-terminally truncated SALL1 proteins in Townes-Brocks syndrome probably dimerize with SALL4 in a dominant-negative manner, resulting in mislocalization of SALL4 in the heterochromatin. Considering the anal and heart anomalies and exencephaly in *Sall1/4* double heterozygotes, the phenotypes observed in Sall1 truncations could be explained by the functional reduction of Sall4.

DISCUSSION

In this study, we showed that mouse *Sall4* is essential for early embryogenesis and for proliferation of ES cells. We also provided both in vivo and in vitro evidence for the dimerization of Sall4 and Sall1 and revealed that the C-terminally truncated Sall1 in Townes-Brocks syndrome caused mislocalization of Sall4 in a dominant-negative manner. As human *SALL4* is a causative gene for the Okihiro syndrome, characterized by limb deformity and eye movement abnormalities, the indispensable role of mouse *Sall4* in early embryogenesis and proliferation of ES cells was entirely unexpected. Blastocyst culture analysis combined with the trophectoderm removal technique identified the importance of *Sall4* in the inner cell mass that

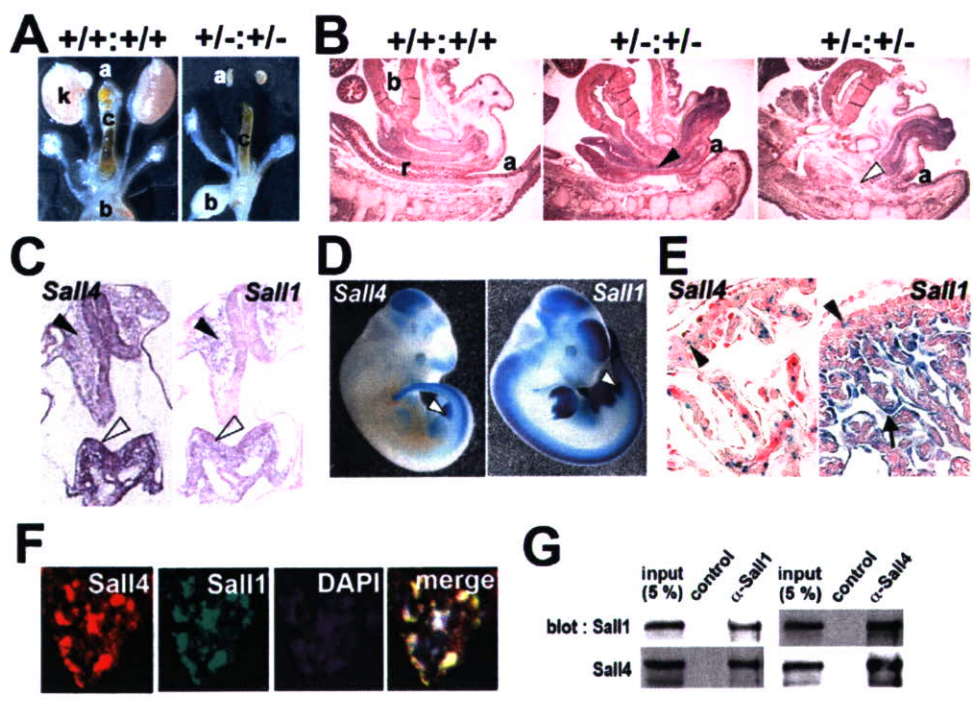

Fig. 5. Genetic interactions of *Sall4* and *Sall1*. (**A**) Bilateral renal agenesis in *Sall1/4* heterozygotes. Six out of the 38 compound heterozygotes analyzed had this phenotype, while 10 had unilateral agenesis. a, adrenal glands; b, urinary bladder; c, colon; k, kidney. (**B**) Anal stenosis in *Sall1/4* heterozygotes at E17.5 (right two panels). Black arrowhead shows complete stenosis of the rectoanal junction; white arrowhead shows absence of the rectum. a, anus; b, urinary bladder; r, rectum. (**C**) In situ hybridization of *Sall4* and *Sall1* at E8.5. The upper side is the anterior region of the embryo (transverse section). Black and white arrowheads indicate the mesenchyme and neuroepithelium, respectively. (**D**) *Sall4* and *Sall1* expression in the anorectal region at E11.5 (arrowheads). Heterozygotes of *Sall4-βgeo* and *Sall1-lacZ* (Nishinakamura et al., 2001) were stained using X-gal. (**E**) Overlap of *Sall4* and *Sall1* in the developing heart at E11.5. *Sall4* is expressed in myocardium (arrowhead), while *Sall1* is expressed in myocardium (arrowhead) and endocardium (arrow). *Sall4-βgeo* and *Sall1-lacZ* mice were stained using X-gal. (**F**) Immunocytochemistry of Sall4 and Sall1, and counterstaining with DAPI in ES cells. (**G**) Binding of Sall4 and Sall1 shown by immunoprecipitation using ES cell lysates.

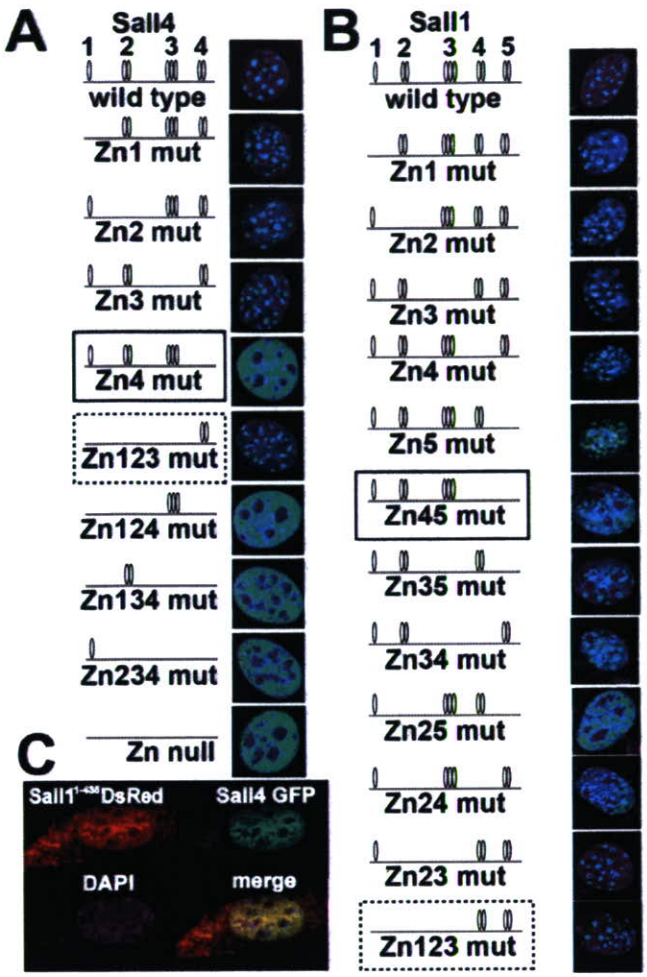

Fig. 6. Mislocalization of Sall4 from the heterochromatin by a truncated Sall1 that functions in a dominant-negative manner. (**A**) Requirement of the C-terminal zinc finger (Zn4) of Sall4 for heterochromatin localization (rectangle). Zn4 is also sufficient for heterochromatin localization (broken outline). Mutants of Sall4-GFP fusion were expressed in NIH 3T3 cells. Zinc-finger clusters are categorized as Zn1, Zn2, Zn3 and Zn4, as shown. (**B**) Requirement of the C-terminal zinc fingers (Zn4 and Zn5) of Sall1 for heterochromatin localization (rectangle). Zn4 and Zn5 are also sufficient for heterochromatin localization (broken outline). Mutations in Zn2 and Zn5 also show a defect in heterochromatin localization, though these two clusters are not sufficient for proper localization in the heterochromatin. (**C**) Co-transfection of truncated *Sall1* (*Sall1*$^{1-435}$-*DsRed*) and *Sall4-GFP* into NIH 3T3 cells. Heterochromatin localization of Sall4 is disrupted by C-terminally truncated Sall1.

is the origin of the embryo proper. As ES cells are derived from the inner cell mass, it is understandable that *Sall4*-null ES cells showed significantly reduced proliferation, which may possibly explain the phenotypes observed in blastocyst culture and embryos in vivo.

How can Sall4 regulate the proliferation of ES cells? As Sall1 is localized in the heterochromatin and binds to the components of chromatin remodeling complexes [namely HDAC1, HDAC2, RbAp46/48, MTA1 and MTA2 (Kiefer et al., 2002)], Sall4 could also bind HDAC complexes and deacetylate the histone lysine residues, followed by recruitment of histone-methylating and DNA-methylating complexes. Centromeric and pericentromeric regions, which comprise constitutive heterochromatin, are required for spindle formation in mitosis, and it is possible that the absence of Sall4 affects these structures. Alternatively, Sall4 could suppress downstream genes, including cell cycle inhibitors, by inducing heterochromatin formation in the euchromatic promoters (known as facultative heterochromatin formation). More detailed examination in the heterochromatin structure in *Sall4* mutant ES cells, as well as identification of downstream target genes of Sall4, is required for further elucidation of Sall4 functions. It is interesting that *Nanog* and *Eras* were slightly decreased in *Sall4*-deficient cells. *Nanog* heterozygous cells show no reduction in proliferation, and *Nanog*-deficient cells differentiate into primitive endoderm (Mitsui et al., 2003). Though *Eras* could be partly responsible for impaired proliferation of *Sall4*-null ES cells, *Eras*-null mice had no abnormalities in vivo (Takahashi et al., 2003). Thus, it is unlikely that a reduction of these genes could explain the phenotypes of *Sall4* deficiency. As ES cells are suitable for quantitative biochemical approaches, we expect to apply the detailed analysis of Sall4 function in ES cells to the study of organ formation during later stages of development.

We demonstrated that Sall4 and Sall1 form heterodimers and that truncated Sall1 proteins altered Sall4 localization in a dominant-negative manner. Townes-Brocks syndrome caused by *SALL1* mutations exhibits limb, anal, ear, kidney and heart anomalies, and mice retaining truncated Sall1 proteins show similar phenotypes as well as exencephaly. As human families with severe phenotypes are unlikely to survive, exencephaly could be one of the phenotypes of SALL1 truncations. Considering the anal and heart anomalies and exencephaly in *Sall1/4* double heterozygotes, at least these three phenotypes observed in Sall1 truncations can be explained by the functional reduction of Sall4. Thus, we propose that some symptoms of Townes-Brocks syndrome caused by SALL1 truncations result from the inhibition of SALL4 functions that is due to heterodimer formation.

SALL4 mutations in humans cause the autosomal dominant disorder Okihiro syndrome, which is characterized by limb deformity, eye movement (abducens nerve) abnormalities, and anorectal, ear, heart, and kidney anomalies. Some *Sall4* heterozygous mice had anal and heart anomalies, suggesting that these phenotypes are caused by *Sall4* haploinsufficiency. This is important because most phenotypes in Townes-Brocks syndrome could be caused by the dominant-negative effect of the truncated Sall1, but not by haploinsufficiency of Sall1. However, other anomalies to limbs, abducens nuclei, inner ears and kidneys were not detected in *Sall4* heterozygous mice; thus, these phenotypes are not explained by *Sall4* haploinsufficiency in mice. In humans, C-terminally truncated SALL4 proteins could function in a dominant-negative manner, as is the case for SALL1 truncations. Recently, a gene trap allele retaining truncated *Sall4* was reported and this strain exhibited digit and heart anomalies (Koshiba-Takeuchi et al., 2006). If this allele serves as a dominant-negative form, it is possible that this trap allele has more severe phenotypes than ours, although other phenotypes are not described. Direct comparison of the two mouse strains on the same genetic background would test this possibility.

We thank H. Niwa for providing the plasmids (*IRES-βgeo*, *IRES-Hyg*, *Oct3/4* and *H19*) and antisera against Oct3/4; H. Suemori, for the anti-mouse antibody for immunosurgery; A. P. Monaghan for providing *Sall3*-deficient mice; H. Masai, M. Nakao, T. Aoto and K. Okita for technical advice; N. Takeda, Y. Kataoka, H. Meguro, S. Yamada, A. Nakane and R. Sakamoto for technical assistance; and T. Hara for critical reading of the manuscript. This work was supported in part by the Ministry of Education, Culture, Sports, Science, and Technology; and by the Ministry of Health, Labor, and Welfare of Japan.

Supplementary material

Supplementary material for this article is available at
http://dev.biologists.org/cgi/content/full/133/15/3005/DC1

References

Al-Baradie, R., Yamada, K., St Hilaire, C., Chan, W. M., Andrews, C., McIntosh, N., Nakano, M., Martonyi, E. J., Raymond, W. R., Okumura, S. et al. (2002). Duane radial ray syndrome (Okihiro syndrome) maps to 20q13 and results from mutations in *SALL4*, a new member of the *SAL* family. *Am. J. Hum. Genet.* **71**, 1195-1199.

Chambers, I., Colby, D., Robertson, M., Nichols, J., Lee, S., Tweedie, S. and Smith, A. (2003). Functional expression cloning of Nanog, a pluripotency sustaining factor in embryonic stem cells. *Cell* **113**, 643-655.

de Celis, J. F., Barrio, R. and Kafatos, F. C. (1996). A gene complex acting downstream of dpp in *Drosophila* wing morphogenesis. *Nature* **381**, 421-424.

de Celis, J. F., Barrio, R. and Kafatos, F. C. (1999). Regulation of the *spalt/spalt-related* gene complex and its function during sensory organ development in the *Drosophila* thorax. *Development* **126**, 2653-2662.

Jurgens, G. (1998). Head and tail development of the *Drosophila* embryo involves *spalt*, a novel homeotic gene. *EMBO J.* **7**, 189-196.

Kiefer, S. M., McDill, B. W., Yang, J. and Rauchman, M. (2002). Murine Sall1 represses transcription by recruiting a histone deacetylase complex. *J. Biol. Chem.* **277**, 14869-14876.

Kiefer, S. M., Ohlemiller, K. K., Yang, J., McDill, B. W., Kohlhase, J. and Rauchman, M. (2003). Expression of a truncated Sall1 transcriptional repressor is responsible for Townes-Brocks syndrome birth defects. *Hum. Mol. Genet.* **12**, 2221-2227.

Kim, J. M., Nakao, K., Nakamura, K., Saito, I., Katsuki, M., Arai, K. and Masai, H. (2002). Inactivation of Cdc7 kinase in mouse ES cells results in S-phase arrest and p53-dependent cell death. *EMBO J.* **21**, 2168-2179.

Kohlhase, J., Wischermann, A., Reichenbach, H., Froster, U. and Engel, W. (1998). Mutations in the *SALL1* putative transcription factor gene cause Townes-Brocks syndrome. *Nat. Genet.* **18**, 81-83.

Kohlhase, J., Hausmann, S., Stojmenovic, G., Dixkens, C., Bink, K., Schulz-Schaeffer, W., Altmann, M. and Engel, W. (1999). *SALL3*, a new member of the human *spalt*-like gene family, maps to 18q23. *Genomics* **62**, 216-222.

Kohlhase, J., Heinrich, M., Schubert, L., Liebers, M., Kispert, A., Laccone, F., Turnpenny, P., Winter, R. M. and Reardon, W. (2002). Okihiro syndrome is caused by *SALL4* mutations. *Hum. Mol. Genet.* **11**, 2979-2987.

Koshiba-Takeuchi, K., Takeuchi, J. K., Arruda, E. P., Kathiriya, I. S., Mo, R., Hui, C. C., Srivastava, D. and Bruneau, B. G. (2006). Cooperative and antagonistic interactions between Sall4 and Tbx5 pattern the mouse limb and heart. *Nat. Genet.* **38**, 175-183.

Kuhnlein, R. P. and Schuh, R. (1996). Dual function of the region-specific homeotic gene *spalt* during *Drosophila* tracheal system development. *Development* **122**, 2215-2223.

Kuhnlein, R. P., Frommer, G., Friedrich, M., Gonzalez-Gaitan, M., Weber, A., Wagner-Bernholz, J. F., Gehring, W. J., Jackle, H and Schuh, R. (1994). *spalt* encodes an evolutionarily conserved zinc finger protein of novel structure which provides homeotic gene function in the head and tail region of the *Drosophila* embryo. *EMBO J.* **13**, 168-179.

Li, D., Dower, K., Ma, Y., Tian, Y. and Benjamin, T. L. (2001). A tumor host range selection procedure identifies p150(sal2) as a target of polyoma virus large T antigen. *Proc. Natl. Acad. Sci. USA* **98**, 14619-14624.

Li, D., Tian, Y., Ma, Y. and Benjamin, T. (2004). p150 (Sal2) is a p53-independent regulator of p21 (WAF1/CIP). *Mol. Cell. Biol.* **24**, 3885-3893.

Matsuda, T., Nakamura, T., Nakao, K., Arai, T., Katsuki, M., Heike, T. and Yokota, T. (1999). STAT3 activation is sufficient to maintain an undifferentiated state of mouse embryonic stem cells. *EMBO J.* **18**, 4261-4269.

Mitsui, K., Tokuzawa, Y., Itoh, H., Segawa, K., Murakami, M., Takahashi, K., Maruyama, M., Maeda, M. and Yamanaka, S. (2003). The homeoprotein Nanog is required for maintenance of pluripotency in mouse epiblast and ES cells. *Cell* **113**, 631-642.

Nellen, D., Burke, R., Struhl, G. and Basler, K. (1996). Direct and long-range action of a DPP morphogen gradient. *Cell* **85**, 357-368.

Nichols, J., Zevnik, B., Anastassiadis, K., Niwa, H., Klewe-Nebenius, D., Chambers, I., Scholer, H. and Smith, A. (1998). Formation of pluripotent stem cells in the mammalian embryo depends on the POU transcription factor Oct 4. *Cell* **95**, 379-391.

Nishimoto, M., Miyagi, S., Yamagishi, T., Sakaguchi, T., Niwa, H., Muramatsu, M. and Okuda, A. (2005). Oct-3/4 maintains the proliferative embryonic stem cell state via specific binding to a variant octamer sequence in the regulatory region of the *UTF1* locus. *Mol. Cell. Biol.* **25**, 5084-5094.

Nishinakamura, R., Matsumoto, Y., Nakao, K., Nakamura, K., Sato, A., Copeland, N. G., Gilbert, D. J., Jenkins, N. A., Scully, S., Lacey, D. L. et al. (2001). Murine homolog of *SALL1* is essential for ureteric bud invasion in kidney development. *Development* **128**, 3105-3115.

Niwa, H., Yamamura, K. and Miyazaki, J. (1991). Efficient selection for high-expression transfectants with a novel eukaryotic vector. *Gene* **108**, 193-200.

Niwa, H., Burdon, T., Chambers, I. and Smith, A. (1998). Self-renewal of pluripotent embryonic stem cells is mediated via activation of STAT3. *Genes Dev.* **12**, 2048-2060.

Niwa, H., Toyooka, Y., Shimosato, D., Strumpf, D., Takahashi, K., Yagi, R. and Rossant, J. (2005). Interaction between Oct3/4 and Cdx2 determines trophectoderm differentiation. *Cell* **123**, 917-929.

Parrish, M., Ott, T., Lance-Jones, C., Schuetz, G., Schwaeger-Nickolenko, A. and Monaghan, A. P. (2004). Loss of the *Sall3* gene leads to palate deficiency, abnormalities in cranial nerves, and perinatal lethality. *Mol. Cell. Biol.* **24**, 7102-7112.

Sato, A., Matsumoto, Y., Koide, U., Kataoka, Y., Yoshida, N., Yokota, T., Asashima, M. and Nishinakamura, R. (2003). Zinc finger protein Sall2 is not essential for embryonic and kidney development. *Mol. Cell. Biol.* **23**, 62-69.

Sato, A., Kishida, S., Tanaka, T., Kikuchi, A., Kodama, T., Asashima, M. and Nishinakamura, R. (2004). Sall1, a causative gene for Townes-Brocks syndrome, enhances the canonical Wnt signaling by localizing to heterochromatin. *Biochem. Biophys. Res. Commun.* **319**, 103-113.

Strathdee, G., Sutherland, R., Jonsson, J. J., Sataloff, R., Kohonen-Corish, M., Grady, D. and Overhauser, J. (1997). Molecular characterization of patients with 18q23 deletions. *Am. J. Hum. Genet.* **60**, 860-868.

Takahashi, K., Mitsui, K. and Yamanaka, S. (2003). Role of ERas in promoting tumour-like properties in mouse embryonic stem cells. *Nature* **423**, 541-545.

Tucker, K. L., Wang, Y., Dausman, J. and Jaenisch, R. (1997). A transgenic mouse strain expressing four drug-selectable marker genes. *Nucleic Acids Res.* **25**, 3745-3746.

Ying, Q. L., Nichols, J., Chambers, I. and Smith, A. (2003). BMP induction of Id proteins suppresses differentiation and sustains embryonic stem cell self-renewal in collaboration with STAT3. *Cell* **115**, 281-292.

J. Physiol. Sci. Vol. 56, No. 2; Apr. 2006; pp. 131–136
Online Apr. 22, 2006; doi:10.2170/physiolsci.M95

Essential Roles of *Sall* Family Genes in Kidney Development

Ryuichi NISHINAKAMURA and Kenji OSAFUNE
Division of Integrative Cell Biology, Institute of Molecular Embryology and Genetics, Kumamoto University, Kumamoto, 860-0811, Japan

Abstract: We isolated a mouse *Sall1*, a mammalian homologue of the *Drosophila* region-specific homeotic gene *spalt* (*sal*), and found that mice deficient in *Sall1* die in the perinatal period from kidney agenesis. *Sall1* is expressed in the metanephric mesenchyme surrounding the ureteric bud, and the homozygous deletion of *Sall1* results in an incomplete ureteric bud outgrowth. Therefore *Sall1* is essential for ureteric bud invasion, the initial key step for metanephros development. We also set up an in vitro culture system, using NIH3T3 cells stably expressing *Wnt4* as a feeder layer, to identify kidney progenitors in the metanephric mesenchyme. In this culture condition, a single renal progenitor in the mesenchyme forms colonies consisting of several types of epithelial cells that exist in glomeruli and renal tubules. We found that only cells strongly expressing *Sall1* (*Sall1-GFP^{high}* cells) form colonies and that they reconstitute a three-dimensional kidney structure in an organ culture setting. Thus our colony-forming assay, which identifies multipotent progenitors in the embryonic mouse kidney, can be used for examining mechanisms of renal progenitor differentiation.

Key words: kidney, development, *Sall1*, metanephric mesenchyme, progenitor.

Three kidneys during development

The kidney function is impaired in a variety of disease states, but all existing treatments for kidney diseases are conservative, and there is essentially no therapy available for curing renal function per se. Regenerating kidney should be tough, but the hints are likely to lie in kidney development. We wish to challenge this difficult project to reveal the mechanisms of kidney development and would like to link the information to strategies for regenerating kidney.

The kidney develops in three stages: pronephros, mesonephros, and metanephros. The nephric duct (Wolffian duct) develops in the craniocaudal direction from the intermediate mesoderm and acts on the surrounding mesenchyme as an inducer of epithelial transformation to nephric tubules. The pronephric and mesonephric tubules and the anterior portion of the Wolffian duct eventually degenerate, and in mammals the metanephros becomes the permanent kidney. Although the pronephros represents a true excretory organ in fish and amphibians, it remains a rudimentary and transient structure in mouse.

Using frog embryos to identify *Sall* genes

The animal cap is a tiny portion of the presumptive ectoderm of *Xenopus* embryos in the blastula stage. In the presence of activin, animal caps differentiate into a variety of tissues. A combination of activin plus retinoic acid induces pronephric tubules efficiently and selectively [1]. We used this animal cap system to identify molecules expressed in pronephros and potentially in mesonephros and metanephros. Thousands of animal caps treated with activin plus retinoic acid were collected at various time points and subjected to a variety of subtraction procedures (Fig. 1). One of the obtained molecules was *Xsal-3*, which is homologous to the *Drosophila* region-specific homeotic gene *spalt* (*sal*) and has multiple double-zinc finger motifs that are characteristic of the *sal* gene family [2]. We also isolated a mouse homologue (*Sall1*) and found it to be expressed in otic vesicles, limb buds, anus, hearts, and kidneys (metanephric mesenchyme) [3].

Drosophila sal is the region-specific homeotic gene characterized by unique multiple double-zinc finger motifs. First identified by virtue of its capacity to promote terminal differentiation, *sal* is expressed in anterior and posterior compartments of *Drosophila,* and mutations in *sal* cause head and tail segments to develop trunk structures [4]. It also plays a critical role in wing development and is expressed at the anterior/posterior boundary of wing imaginal discs. Its expression is controlled by *dpp* (BMP-4 orthologue), the expression of which is highest at the boundary, which in turn is controlled by *hedgehog,* expressed in the posterior compartment [5]. An overexpression of *dpp* broadens the expression domains of *sal*; thus *sal* may be a downstream target of *dpp*. It was also found to be downstream of the *wingless* signal in the *Drosophila* tracheal system, and *sal* deletion results in an absence of dorsal trunks of the trachea [6].

Received on Nov 22, 2005; accepted on Apr 19, 2006; released online on Apr 22, 2006; doi:10.2170/physiolsci.M95
Correspondence should be addressed to: Ryuichi Nishinakamura, Division of Integrative Cell Biology, Institute of Molecular Embryology and Genetics, Kumamoto University, 2-2-1 Honjo, Kumamoto, 860-0811, Japan Phone: +81-96-373-6615, Fax: +81-96-373-6618, E-mail: ryuichi@kaiju.medic.kumamoto-u.ac.jp

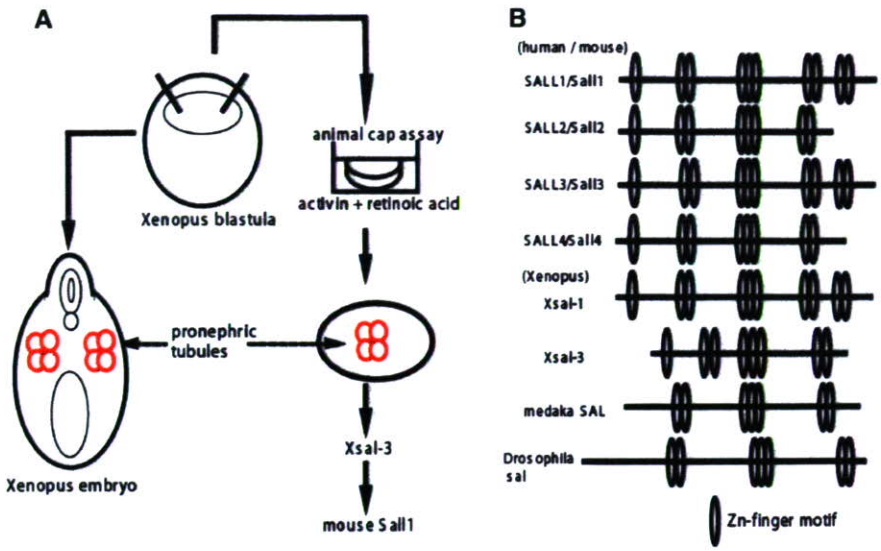

Fig. 1. Pronephros formation in animal caps in *Xenopus laevis* and cloning of *Sall* genes. **A**: Pronephros formation in animal caps treated with activin plus retinoic acid. Animal caps treated for three hours contain pronephric tubules 3 days after the treatment. **B**: *Sall* family genes conserved from *Drosophila* to humans. Ovals indicate zinc-finger motifs.

Sall1 is essential to kidney development

In metanephros development, the metanephric mesenchyme induces a sprouting of the ureteric bud from the caudal region of the Wolffian duct (Fig. 2). Signals from the mesenchyme cause a further branching of the ureteric bud, thus forming the collecting ducts and the ureters. Reciprocally, the ureteric bud invades the mesenchyme and induces epithelialization and differentiation of the mesenchyme into the glomeruli, the loop of Henle, and the proximal and distal tubules.

When we generated *Sall1* knockout mice, all of the homozygous mice died within 24 hours after birth, and kidney agenesis or severe dysgenesis was present (Fig. 3) [3]. About a third had no kidneys or ureters bilaterally (Fig. 3B). The remaining mice had either unilateral kidney agenesis or bilateral hypolasia (Fig. 3C). At day 11.5 of gestation (E11.5), the ureteric bud invades the metanephric mesenchyme, and subsequent reciprocal interaction between these two tissues leads to a development of a metanephric kidney (Fig. 3D). In *Sall1*-null mice, morphologically distinct metanephric mesenchyme was formed, though the size was reduced (Fig. 3E). In contrast, the ureteric bud formed, but failed to invade the metanephric mesenchyme. Thus a loss of *Sall1* leads to a failure of ureteric bud invasion into the mesenchyme, the initial key step for metanephros development. The development of other organs, including brain, adrenal glands, bladder, testis, and ovary, was normal.

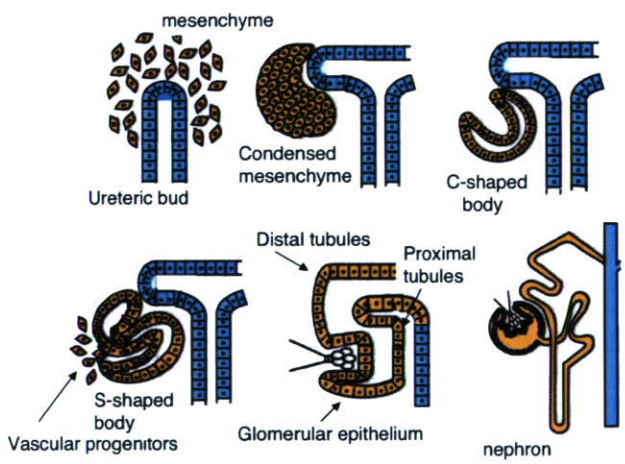

Fig. 2. Metanephros development. See details in the text. The mesenchyme gives rise to the glomeruli, proximal and distal tubules, and the loops of Henle, but the ureteric bud differentiates into the collecting ducts and the ureters. *Sall1* is expressed in the mesenchyme and is essential for the ureteric bud attraction to the mesenchyme.

Molecular mechanisms of kidney development

The molecular mechanisms of kidney development have been revealed mostly by gene targeting. Here I briefly introduce some of the findings (Fig. 4), but more-detailed reviews are also available [7, 8]. A member of the TGF-β superfamily, GDNF (glial cell-line-derived neurotrophic factor), expressed in the mesenchyme, acts on a receptor tyrosine kinase Ret distributed in the ureteric bud epithelium and induces a branching of the ureter. Thus the null mutants of *GDNF* and *Ret* show perturbation of ureter invasion. The transcription factors Six1, Pax2, and Eya1 also control kidney development, partly by upregulating *GDNF* expression. In contrast, secreted proteins Slit2 and BMP4 antagonize the GDNF action and inhibit the ectopic formation of ureteric buds.

Reciprocal signals from the ureteric bud to the mesenchyme remained unidentified for a long period. Recently, Wnt9b was reported to be a ureter-derived regulator for mesenchymal to epithelial conversion, and mice that are deficient in Wnt9b lack the initial induction of the mesenchyme, including Wnt4 expression [9]. Mice lacking Wnt-4 fail to form pretubular aggregates, a transitional

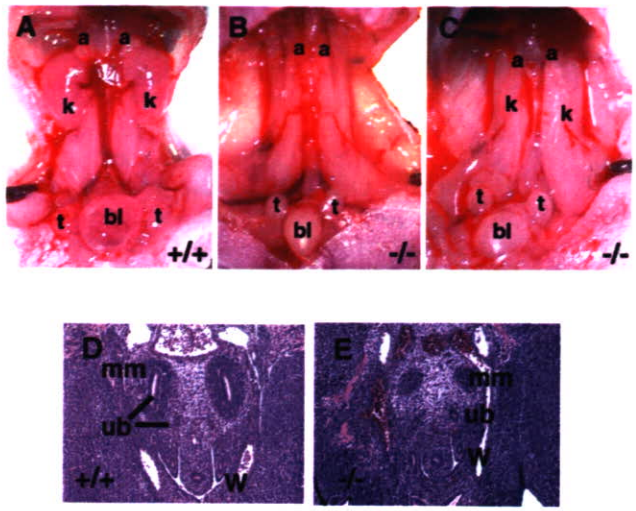

Fig. 3. Kidney phenotypes in *Sall*1-deficient mice. **A**: Kidneys (k) of wild-type newborn. Urinary bladder (bl) is filled with urine. **B**: Kidneys of *Sall1*-deficient newborn. Note that kidneys are absent and the urinary bladder is not inflated with urine. Other organs, such as adrenal glands (a) and testes (t), are normal. **C**: Kidneys of another *Sall1*-deficient newborn with severe bilateral kidney hypoplasia. Urine is absent in the bladder. **D**: Metanephros in wild-type mice at 11.5 dpc. The ureteric bud (ub) branches from the Wolffian duct (W) and metanephric mesenchymes (mm) are condensed around the bulging ureteric bud. **E**: Metanephros in *Sall1*-deficient mice at 11.5 dpc. The metanephric mesenchyme is formed, but it is reduced in size and is not invaded by the ureteric bud.

state from mesenchyme to tubules; thus Wnt4 functions downstream of Wnt9b and acts as an autoinducer of the mesenchyme to epithelial transition.

Potential mechanisms related to the *Sall* family

Several possibilities can explain the *Sall1* knockout phenotype. Soluble factors secreted from the mesenchyme to attract the ureteric bud may be impaired in the absence of *Sall1*. GDNF is a potential candidate, and indeed the most severe cases in *Sall1* knockout were similar to those seen in *GDNF*-deficient mice. *GDNF* is expressed in the metanephric mesenchyme and is a key molecule for attracting the ureteric bud, acting through the Ret receptor. *GDNF* expression in the mesenchyme is reduced in *Sall1* knockout at E11.5, but not at E10.5 (before ureteric bud invasion). Therefore *Sall1* is not absolutely required for *GDNF* expression. It is, however, still possible that reduced levels of GDNF may explain the ureteric bud phenotype of *Sall1* knockout.

It was reported that Sall1 also functions as a transcriptional repressor by localizing in the heterochromatin and interacting with the components of chromatin remodeling complexes, such as histone deacetylase (HDAC)1, HDAC2, retinoblastoma-associated protein 46/48 (RbAp46/48), metastasis-associated protein (MTA)1, and MTA2 [10, 11]. *Sall1* may bind to heterochromatin directly and recruit molecules that form heterochromatin complexes. If this hypothesis is valid, *Sall1* may repress inhibitors, thereby activating kidney development. Direct targets that are repressed by *Sall1* remain unknown, and the identification of such targets is needed to fully explain kidney phenotypes of *Sall1*-deficient mice. *Sall1* contains 10 zinc finger motifs, most of which are clustered in duplex or triplet, but it is not known which zinc finger domain is involved in DNA binding or in transactivation. A search for *Sall1* target genes is under way in various laboratories.

Kidney abnormalities caused by human *SALL1* mutations

Humans and mice have four known *sal*-related genes, respectively (*SALL1-4* for humans and *Sall1-4* for mice). Mutations in *SALL1* have been associated with Townes-Brocks syndrome, an autosomal dominant disease with features of dysplastic ears, preaxial polydactyly, imperforate anus, and, less commonly, kidney and heart anomalies [12]. Mice deficient in *Sall1* show kidney agenesis or severe dysgenesis, but other phenotypes observed in human disease are not apparent, as described above [3]. This discrepancy could be explained by truncated SALL1 proteins resulting from human mutations, possibly functioning in a dominant-negative manner, because mutant mice

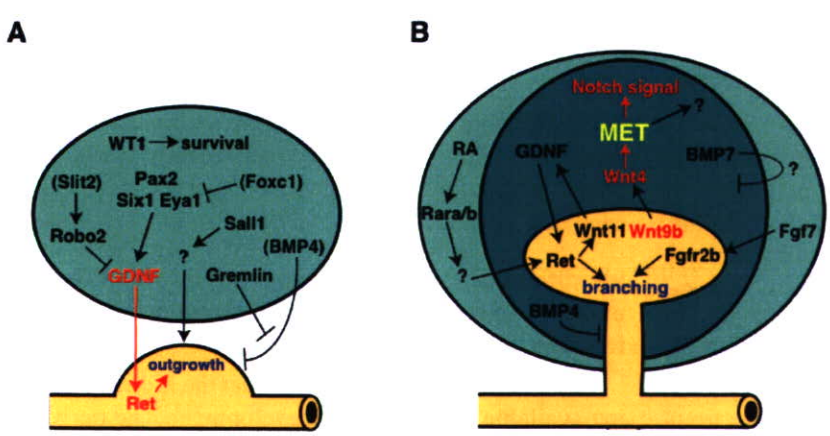

Fig. 4. Molecules involved in kidney development. **A**: Mesenchyme secretes GDNF and attracts the ureterid bud. **B**: Wnt9b secreted from the ureteric bud upregulates Wnt4 in the mesenchyme. Wnt4 in turn plays a role in mesenchymal-to-epithelial transition (MET).

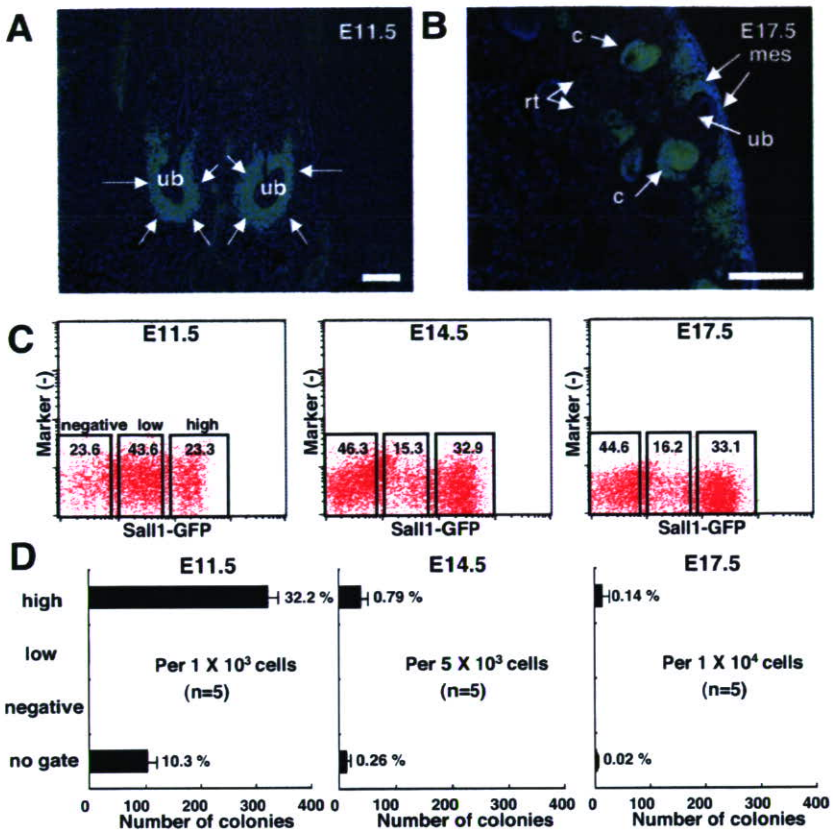

Fig. 5. Colony-forming progenitors exist in the *Sall1-GFP^{high}* subpopulation of the metanephros. **A, B**: Cryosections of the metanephros of *Sall1-GFP* knock-in mouse (A: E11.5, B: E17.5). ub: ureteric bud; mes: mesenchyme; c: C-shaped body; rt: renal tubule; blue: DAPI. Scale bars: 50 μm. **C**. Metanephros contains three subpopulations (*Sall1-GFP^{high}*, *Sall1-GFP^{low}*, and *Sall1-GFP^{negative}*). The percentages of the subpopulations at each fetal stage are shown. **D**. Numbers of colonies in each subpopulation derived from E11.5 mesenchyme, E14.5, and E17.5 metanephros. The number of colonies were counted after a 20-day culture.

that produce a truncated Sall1 protein exhibit more severe defects than *Sall1*-null mice, including renal agenesis, exencephaly, and limb and anal deformities [13]. *Sall2*-deficient mice show no apparent phenotypes, and mice lacking both *Sall1* and *Sall2* show kidney phenotypes comparable to those of *Sall1* knockout [14]. *Sall3*-null mice die on the first postnatal day, and deficiencies in cranial nerves and abnormalities in the oral structures are present [15]. Mutations of *SALL4* cause an autosomal dominant disorder, Okihiro syndrome, characterized by limb deformity and eye movement deficits and, though less common, anorectal and kidney anomalies [16, 17], and we are currently generating *Sall4*-deficient mice. A generation of mice lacking all *Sall* genes would be necessary to address the developmental roles of the *Sall* family.

Identification of kidney mesenchymal genes by a combination of microarray analysis and *Sall1-GFP* knock-in mice

Gene targeting has revealed several genes essential to kidney development, yet more genes are probably involved in the generation of a complicated kidney. In the embryonic kidney, *Sall1* is expressed abundantly in mesenchyme-derived structures from condensed mesenchyme and S- and comma-shaped bodies to renal tubules and podocytes. We generated mice in which a green fluorescent protein (*GFP*) gene was inserted into the *Sall1* locus, and we isolated the *GFP*-positive population from embryonic kidneys of these mice by fluorescein-activated cell sorting (FACS) [18]. The *GFP*-positive population indeed expressed mesenchymal genes, but the negative population expressed genes in the ureteric bud. To systematically search for genes expressed in the mesenchyme-derived cells, we compared gene expression profiles in the *GFP*-positive and *GFP*-negative populations by using microarray analysis followed by in situ hybridization. We detected many genes known to be important for metanephros development, including *Sall1*, *GDNF*, *Raldh2*, *Pax8*, and *FoxD1*, and genes expressed abundantly in the metanephric mesenchyme, such as *Unc4.1*, *Six2*, *Osr-2*, and *PDGFc*. We also found groups of genes, including *SSB-4*, *Smarcd3*, *μ-Crystallin*, and *TRB-2*, that are not known to be expressed in the metanephric mesenchyme. Therefore a combination of microarray technology and *Sall1-GFP* mice is useful for a systematic identification of genes expressed in the developing kidney. Finding essential genes from this large list requires efficient and rapid screening. siRNA technology has recently become one potent method, but generating the knockout mice of each candidate gene is necessary for proof.

Identification of multipotent progenitors in the embryonic mouse kidney by a novel colony-forming assay

Eventually we hope to reconstruct the kidney by utilizing available knowledge on development. The derivation

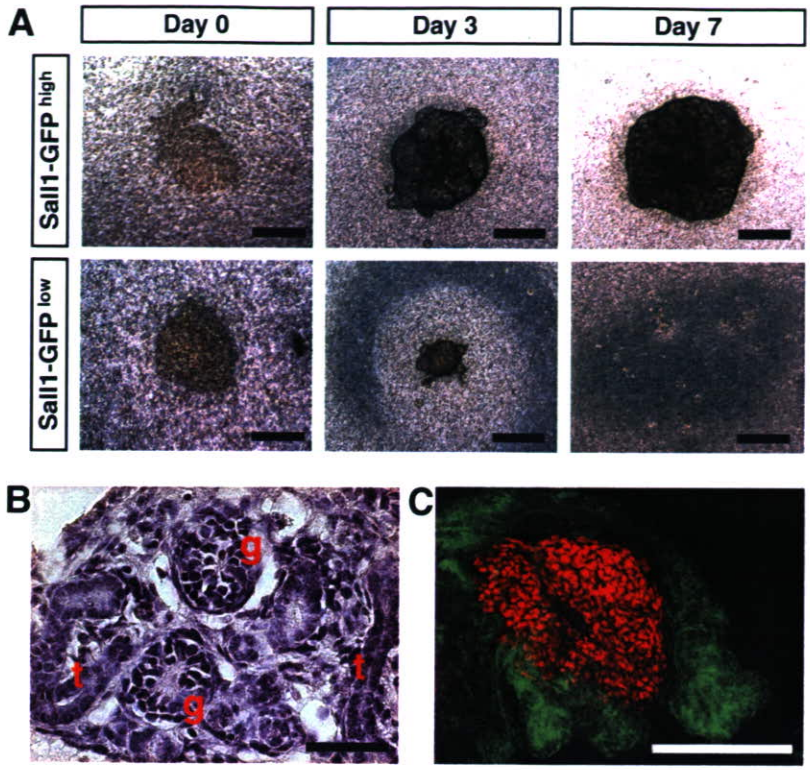

Fig. 6. *Sall1-GFP*^{high} mesenchyme differentiates into renal epithelia in organ culture. **A**: Three subpopulations in E11.5 mesenchyme (*Sall1-GFP*^{high}, *Sall1-GFP*^{low}, and *Sall1-GFP*^{negative}) were cultured on 3T3Wnt4 feeder cells in an organ culture setting. Only *Sall1-GFP*^{high} cells (upper panels) differentiated into the kidney structure; the *Sall1-GFP*^{low} cells (lower) disappeared. **B**: Hematoxylin-eosin staining of sections of *Sall1-GFP*^{high} aggregates at day 10. Tubule- (t) and glomerulus-like structures (g) are seen. **C**: Double staining with WT1 (red, podocyte marker) and LTL (green, proximal tubule marker) of *Sall1-GFP*^{high} aggregates. Scale bars: (A) 500 μm; (B, C) 25 μm.

of kidney cells from a variety of sources such as embryonic stem cells and bone marrow would be a challenge. For this purpose, assay systems that recognize the existence and frequency of kidney progenitors, both in vitro and in vivo, are needed. We established a novel colony-forming assay system by using 3T3 cells expressing *Wnt4* (3T3Wnt4) to identify renal progenitors in the metanephric mesenchyme [19].

We cultured dissociated cells from the metanephric mesenchyme of E11.5 embryos, using 3T3Wnt4 as a feeder layer in a serum-free condition. This culture condition resulted in a formation of sheetlike colonies, and these colonies contain differentiated cells expressing marker genes for epithelia in glomeruli (podocyte), proximal or distal tubules, and the loop of Henle. We also confirmed by clone sorting that these colonies are derived from a single progenitor with multipotent differentiating capacity.

We next attempted to prospectively identify the renal progenitor cells by using *Sall1-GFP* knock-in mice [18]. Because *Sall1* is expressed in mesenchyme-derived tissues, GFP was detected in the mesenchyme around the ureteric bud at E11.5 in the *Sall1-GFP* heterozygous mouse (Fig. 5A, arrows). At E17.5, GFP-expressing cells were observed in the mesenchyme near the surface, as well as in C- or S-shaped bodies and parts of renal tubules (Fig. 5B). By flowcytometrical analysis, three subpopulations were fractionated based on the expression of *Sall1-GFP*: *Sall1-GFP*^{high}, *Sall1-GFP*^{low}, and *Sall1-GFP*^{negative} (Fig. 5C), and the numbers of the colony-forming progenitors in each subpopulation were examined by the use of the low-density culture on 3T3Wnt4 (Fig. 5D). At E11.5, colonies were formed exclusively from *Sall1-GFP*^{high} population, and not from the *Sall1-GFP*^{low} or *Sall1-GFP*^{negative} population. At E14.5 and E17.5, colonies were also formed only from *Sall1-GFP*^{high} subpopulations, but the frequency of colony-forming progenitors decreased as gestation proceeded. These results indicate that renal progenitors with multipotent differentiating capacity are included in cell populations strongly expressing *Sall1* throughout gestation periods.

Sall1-GFP^{high} mesenchyme reconstitutes a three-dimensional structure in organ culture

We examined the in vitro differentiation capacity of three subpopulations in E11.5 mesenchyme by modifying the organ culture of mesenchyme rudiments [19]. *Sall1-GFP*^{high}, *Sall1-GFP*^{low}, and *Sall1-GFP*^{negative} cells were separated by flowcytometry, aggregated to form a cell pellet by centrifugation and cultured on 3T3Wnt4 feeder cells in an organ culture setting. Starting from day 3 in culture, tubulogenesis was observed only in the aggregate of *Sall1-GFP* ^{high} population (Fig. 6A, upper panels), but that from *Sall1-GFP* ^{low} or *Sall1-GFP* ^{negative} did not differentiate and disappeared by day 7 (Fig. 6A, lower panels; data of *Sall1-GFP*^{negative} not shown). In sections of the *Sall1-GFP*^{high} aggregate (Fig. 6B), many tubule- (t) and glomerulus-like structures (g) were observed, and the expression of markers for glomerular podocyte (WT1, Fig.

6C, red) and proximal tubule (LTL, green) was confirmed by confocal microscopy. These data suggest that only *Sall1-GFP*^{high} cells differentiate into renal epithelia in vitro in a three-dimensional setting, besides forming colonies. Thus our colony-forming assay, which identifies multipotent progenitors in the embryonic mouse kidney, can be used for examining the mechanisms of renal progenitor differentiation as well as for the derivation of kidney progenitors from a variety of cell sources.

We thank Minoru Takasato for the initial characterization of *Sall1-GFP* mice and Andreas Kispert for providing 3T3Wnt4 cells.

REFERENCES

1. Uochi T, Asashima M. Sequential gene expression during pronephric tubule formation in vitro in *Xenopus* ectoderm. Dev Growth Differ. 1996;38:625-35.
2. Onuma Y, Nishinakamura R, Takahashi S, Yokota T, Asashima M. Molecular cloning of a novel *Xenopus spalt* gene (*Xsal-3*). Biochem Biophys Res Commun. 1999;264:151-6.
3. Nishinakamura R, Matsumoto Y, Nakao K, Nakamura K, Sato A, Copeland NG, Gilbert DJ, Jenkins NA, Scully S, Lacey DL, Katsuki M, Asashima M, Yokota T: Murine homolog of *SALL1* is essential for ureteric bud invasion in kidney development. Development. 2001;128:3105-15.
4. Kuhnlein RP, Frommer G, Friedrich M, Gonzalez-Gaitan M, Weber A, Wagner-Bernholz JF, Gehring WJ, Jackle H, Schuh R. *spalt* encodes an evolutionarily conserved zinc finger protein of novel structure which provides homeotic gene function in the head and tail region of the *Drosophila* embryo. EMBO J. 1994;13:168-79.
5. de Celis JF, Barrio R, Kafatos FC. A gene complex acting downstream of dpp in *Drosophila* wing morphogenesis. Nature. 1996;381:421-4.
6. Chihara T, Hayashi S. Control of tracheal tubulogenesis by Wingless signaling. Development. 2000;127:4433-4442.
7. Vainio S, Lin Y. Coordinating early kidney development: lessons from gene targeting. Nat Rev Genet. 2002;3:533-43.
8. Perantoni AO. Renal development: perspectives on a Wnt-dependent process. Semin Cell Dev Biol. 2003;14:201-8.
9. Carroll TJ, Park JS, Hayashi S, Majumdar A, McMahon AP. Wnt9b plays a central role in the regulation of mesenchymal to epithelial transitions underlying organogenesis of the mammalian urogenital system. Dev Cell. 2005;9:283-92.
10. Netzer C, Rieger L, Brero A, Zhang CD, Hinzke M, Kohlhase J, Bohlander SK. *SALL1*, the gene mutated in Townes-Brocks syndrome, encodes a transcriptional repressor which interacts with TRF1/PIN2 and localizes to pericentromeric heterochromatin. Hum Mol Genet. 2001;10:3017-24.
11. Kiefer SM, McDill BW, Yang J, Rauchman M. Murine Sall1 represses transcription by recruiting a histone deacetylase complex. J Biol Chem. 2002;277:14869-76.
12. Kohlhase J, Wischermann A, Reichenbach H, Froster U, Engel W. Mutations in the *SALL1* putative transcription factor gene cause Townes-Brocks syndrome. Nat Genet. 1998;18:81-3.
13. Kiefer SM, Ohlemiller KK, Yang J, McDill BW, Kohlhase J, Rauchman M. Expression of a truncated Sall1 transcriptional repressor is responsible for Townes-Brocks syndrome birth defects. Hum Mol Genet. 2003;12:2221-7.
14. Sato A, Matsumoto Y, Koide U, Kataoka Y, Yoshida N, Yokota T, Asashima M, Nishinakamura R. Zinc finger protein Sall2 is not essential for embryonic and kidney development. Mol Cell Biol. 2003;23:62-9.
15. Parrish M, Ott T, Lance-Jones C, Schuetz G, Schwaeger-Nickolenko A, Monaghan AP. Loss of the *Sall3* gene leads to palate deficiency, abnormalities in cranial nerves, and perinatal lethality. Mol Cell Biol. 2004;24:7102-12.
16. Al-Baradie R, Yamada K, St Hilaire C, Chan WM, Andrews C, McIntosh N, Nakano M, Martonyi EJ, Raymond WR, Okumura S, Okihiro MM, Engle EC. Duane radial ray syndrome (Okihiro syndrome) maps to 20q13 and results from mutations in *SALL4*, a new member of the *SAL* family. Am J Hum Genet. 2002;71:1195-9.
17. Kohlhase J, Heinrich M, Schubert L, Liebers M, Kispert A, Laccone F, Tumpenny P, Winter RM, Reardon W. Okihiro syndrome is caused by *SALL4* mutations. Hum Mol Genet. 2002;11:2979-87.
18. Takasato M, Osafune K, Matsumoto Y, Kataoka Y, Yoshida N, Meguro H, Aburatani H, Asashima M, Nishinakamura R. Identification of kidney mesenchymal genes by a combination of microarray analysis and *Sall1-GFP* knockin mice. Mech Dev. 2004;121:547-57.
19. Osafune K, Takasato M, Kispert A, Asashima M, Nishinakamura R. Identification of multipotent progenitors in the embryonic mouse kidney by a novel colony-forming assay. Development. 2006;133:151-61.

Mouse homolog of SALL1, a causative gene for Townes–Brocks syndrome, binds to A/T-rich sequences in pericentric heterochromatin via its C-terminal zinc finger domains

Kazunari Yamashita[1,2,a], Akira Sato[3,4,a], Makoto Asashima[4], Pi-Chao Wang[2] and Ryuichi Nishinakamura[1,3,*]

[1]*Division of Integrative Cell Biology, Institute of Molecular Embryology and Genetics, Kumamoto University, Kumamoto 860-0811, Japan*
[2]*Division of Biological Functional Science, Graduate School of Life and Environmental Science, University of Tsukuba, Ibaraki 305-8572, Japan*
[3]*Division of Stem Cell Regulation, The Institute of Medical Science, The University of Tokyo, Tokyo 108-8639, Japan*
[4]*Department of Life Sciences, The University of Tokyo, Tokyo 153-8902, Japan*

The *Spalt* (*sal*) gene family is conserved from *Drosophila* to humans. Mutations of human *SALL1* cause Townes–Brocks syndrome, with features of ear, limb, anal, renal and heart anomalies. *Sall1*, a murine homolog of *SALL1*, is essential for kidney formation, and both Sall1 and SALL1 localize to heterochromatin in the nucleus. Here, we present a molecular mechanism for the heterochromatin localization of Sall1. Mutation analyses revealed that the 7th–10th C-terminal double zinc finger motifs were required for the localization. A recombinant protein of the most C-terminal double zinc finger (9th–10th) bound to specific A/T-rich sequences. Furthermore, Sall1 associated with A/T-rich sequences of the major satellite DNA in heterochromatin. Thus Sall1 may bind to A/T-rich sequences of the major satellite DNA via its C-terminal double zinc fingers, thereby mediating its localization to heterochromatin.

Introduction

The *Spalt* (*sal*) gene family encodes multiple C2H2-type zinc finger proteins that play important roles in regulating the developmental processes of many organs in *Drosophila* (Reuter *et al.* 1989; de Celis *et al.* 1996; Boube *et al.* 2000; de Celis & Barrio 2000; Elstob *et al.* 2001; Mollereau *et al.* 2001; Rusten *et al.* 2001; Dong *et al.* 2003). Humans have four *sal* homolog genes (*SALL1*, *SALL2*, *SALL3* and *SALL4*), similar to the case for mice (*Sall1*, *Sall2*, *Sall3* and *Sall4*) (Kohlhase *et al.* 1996, 1999, 2000, 2002a,b; Ott *et al.* 1996, 2001; Buck *et al.* 2000, 2001; Al-Baradie *et al.* 2002). Heterozygous mutations of human *SALL1* lead to Townes–Brocks syndrome, with features of dysplastic ears, preaxial polydactyly, imperforate anus, and less commonly, kidney and heart anomalies (Kohlhase *et al.* 1998). Homozygous deletion in mice causes severe kidney defects, indicating that *Sall1* has an essential role in kidney development, although this *Sall1*-null mouse model never mimics the human syndrome (Nishinakamura *et al.* 2001). In contrast, mice carrying a mutant allele that produces a truncated protein recapitulate the abnormalities found in the human disease (Kiefer *et al.* 2003). Mice heterozygous for both *Sall1* and *Sall4* also exhibit some of these abnormalities, including renal, cardiac and anal symptoms (Sakaki-Yumoto *et al.* 2006). Since Sall1 and Sall4 form heterodimers, Sall1 could cooperate with other Sall family members not only in kidney development, but also in the developmental processes of many other organs in mice.

The molecular mechanisms of action of Sall1 and SALL1 are, however, still obscure. Sall1 functions as a transcriptional repressor, as determined by luciferase reporter assays, and interacts physically with histone deacetylase (HDAC) and other components of the chromatin remodeling NuRD complex. However, it remains to be resolved whether the transcriptional repression is solely dependent on the HDAC activity (Netzer *et al.*

Communicated by: Tetsuya Taga
**Correspondence*: E-mail: ryuichi@kaiju.medic.kumamoto-u.ac.jp
[a]These two authors contributed equally to this work.

DOI: 10.1111/j.1365-2443.2007.01042.x

2001; Kiefer *et al.* 2002). Both human SALL1 and mouse Sall1 localize to pericentric heterochromatin (Netzer *et al.* 2001; Kiefer *et al.* 2002; Sato *et al.* 2004), a highly condensed chromatin structure that exists near the centromeric region (Horz & Altenburger 1981; Wong & Rattner 1988). In mouse cells, pericentric heterochromatin is mainly composed of a repetitive DNA sequence called the major satellite repeat, and some proteins, including heterochromatin protein 1 (HP1) that maintain the heterochromatin structure. The histones in this region are highly methylated, especially the 9th lysine of the histone H3 tail (H3K9) (Nielsen *et al.* 2001; Lachner *et al.* 2003; Peters *et al.* 2003). The centromere is known to function in the organization of correct chromosome segregation, whereas the functions of pericentric heterochromatin remain largely unknown. Recently, an association between transcriptional repression and SALL1 localization to heterochromatin was reported (Netzer *et al.* 2006), indicating that the functions of Sall1 may depend on its localization to heterochromatin.

Here, we focused on the zinc finger domains of Sall1, and determined the mechanism of its localization to heterochromatin. *Sall1* encodes a protein that contains ten zinc finger motifs. The most N-terminal zinc finger is a single C2HC-type zinc finger that is only conserved in vertebrates (*Drosophila sal* does not have this N-terminal C2HC zinc finger). The other zinc fingers are of the C2H2-type and arranged as doublets (double zinc fingers) or triplets. We demonstrate that Sall1 requires its C-terminal double zinc finger domains for localization to heterochromatin, and that these domains recognize A/T-rich nucleotide sequences in the major satellite DNA of heterochromatin.

Results

C2H2 zinc finger domains of Sall1 are necessary for its localization to heterochromatin

Over-expressed Sall1 protein has been reported to localize to pericentric heterochromatin in cultured cell lines (Netzer *et al.* 2001; Kiefer *et al.* 2002; Sato *et al.* 2004). However, the localization of endogenous Sall1 remains unclear. Since embryonic stem (ES) cells expressed abundant Sall1 protein as evaluated by Western blot analysis (data not shown), we examined the localization of endogenous Sall1 in ES cells using an anti-Sall1 antibody. Heterochromatin regions can be identified by bright spots of 4,6-diamidino-2-phenylindole (DAPI) staining (DAPI-dense clusters) in the nuclei of several mouse cell lines. We also used anti-HP1α and anti-tri-methylated H3K9 antibodies to visualize the regions of heterochromatin. The staining for Sall1 revealed a dotted pattern in the nucleus that overlapped with the staining for HP1α and tri-methylated H3K9 (Fig. 1A), indicating that endogenous Sall1 is localized to heterochromatin. NIH 3T3 cells do not express Sall1 and serve as a tool for assessing the distribution of exogenous Sall1. When wild-type or GFP-fused Sall1 was introduced into NIH3T3 cells, both proteins localized to heterochromatin (Fig. 1B and data not shown). Thus the Sall1-GFP fusion protein is likely to be useful for dissecting the localization mechanisms of Sall1 to heterochromatin.

To examine whether the zinc finger domains of Sall1 are required for its heterochromatin localization, we produced a GFP-fused full-length Sall1 point mutant (Zn1-5mut), in which the cysteine residues of all the zinc finger domains were replaced by glycine residues (Fig. 1C). Zn1-5mut diffused uniformly throughout the nuclear regions and avoided the spots that were positive for DAPI, tri-methylated H3K9 or HP1α (Fig. 1D; data not shown), indicating that it is not localized to heterochromatin. Zn2-5mut, a similar mutant except for the N-terminal C2HC zinc finger motif, showed a similar localization pattern to Zn1-5mut. In contrast, a Zn1 mutant that retained all the zinc fingers except for the N-terminal one was localized to heterochromatin. These results indicate that four clusters of the C2H2 zinc finger domains of Sall1 (Zn2, Zn3, Zn4 and Zn5) are necessary for the localization, whereas Zn1 is not.

Localization of Sall1 to heterochromatin requires the C-terminal double zinc fingers Zn4 and Zn5

To determine which zinc finger domains of Sall1 are essential for its localization to heterochromatin, we produced a series of mutants (Zn345mut, Zn245mut, Zn235mut and Zn234mut), which each returned one intact zinc finger domain cluster to the mutant Zn2-5mut (Fig. 2A). However, none of these single C2H2 double zinc finger domains completely restored the localization of Sall1 to heterochromatin. Among the mutants, Zn234mut, which had an intact Zn5, partially localized to heterochromatin (Fig. 2A, red box; Fig. 2D), suggesting that Zn5 may be the most responsible cluster for the Sall1 localization. Next, we prepared another series of mutants (Zn45mut, Zn35mut, Zn34mut, Zn25mut, Zn24mut and Zn23mut), which each returned two intact zinc finger clusters to the mutant Zn2-5mut (Fig. 2B). Zn25mut, which had mutations in both Zn2 and Zn5, still diffused uniformly throughout the nucleus except for the spots that were positive for DAPI or tri-methylated H3K9 (Fig. 2B, upper red box; Fig. 2D), while the other four mutants (Zn45mut, Zn35mut,

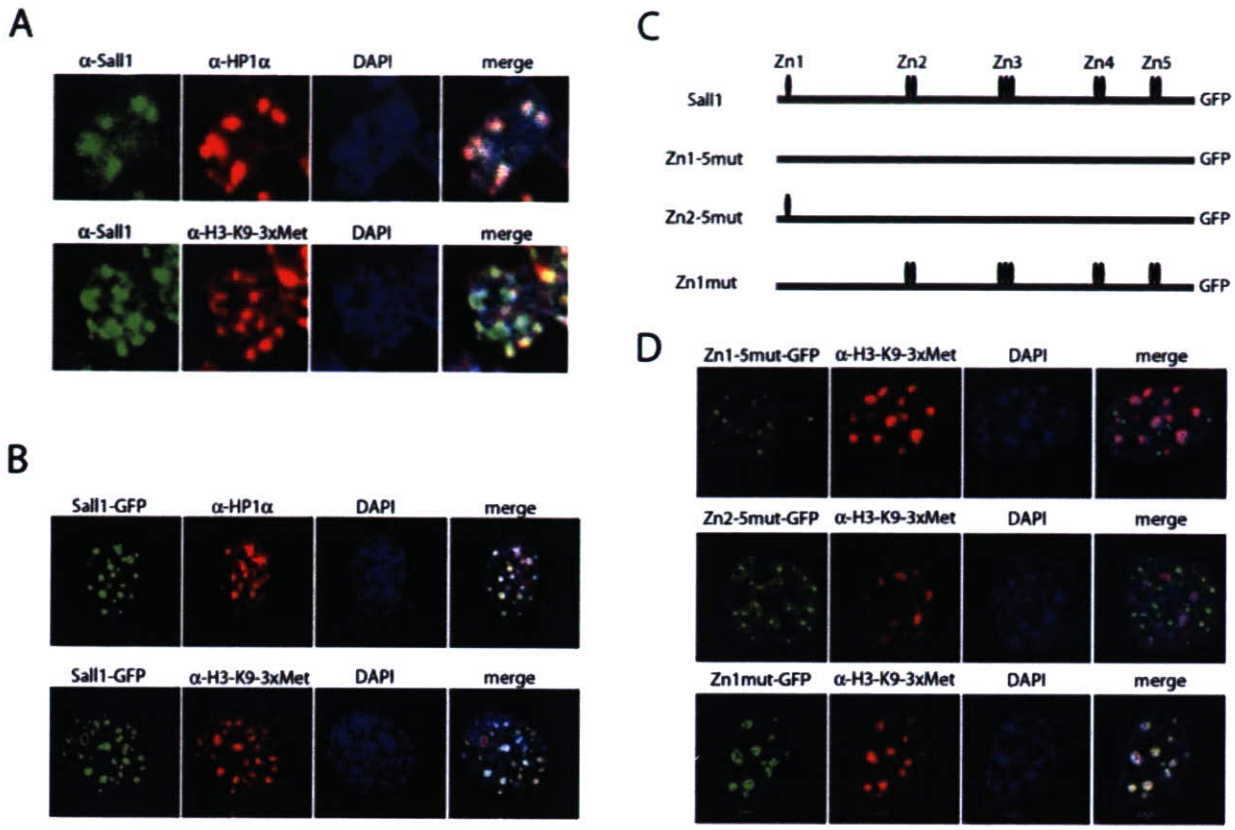

Figure 1 C2H2 zinc finger domains of Sall1 are required for its localization to heterochromatin. (A) Endogenous Sall1 (green) in embryonic stem cells is colocalized with the heterochromatin markers HP1α (red), tri-methylated H3K9 (red) and DAPI staining (blue). (B) Sall1-GFP (green) introduced into NIH3T3 cells are also localized to heterochromatin. (C) Diagrams of GFP-fused full-length Sall1 and zinc finger mutants. The zinc fingers are represented by ovals. (D) Localizations of GFP-fused Sall1 mutants (green) in NIH3T3 cells. Heterochromatin is stained with an anti-tri-methylated H3K9 antibody (red) or DAPI (blue).

Zn34mut and Zn24mut) were partially localized to heterochromatin. Strikingly, Zn23mut, which had intact Zn4 and Zn5 double zinc finger clusters, was completely localized to heterochromatin, similar to the case for wild-type Sall1-GFP (Fig. 2B, lower red box; Fig. 2D). Further disruption of Zn1 (Zn123mut) did not affect the localization. These results suggest that Zn4 and Zn5 are sufficient for heterochromatin localization. Next, we constructed mutants in which only one zinc finger cluster was mutated. Although mutations in Zn2 or Zn3 had no effects, mutations in either Zn4 or Zn5, especially Zn5, caused localization not only in heterochromatin but also in other nuclear regions that were negative for DAPI or tri-methylated H3K9 (Fig. 2C, red box; Fig. 2D). Thus the C-terminal two zinc finger clusters (Zn4 and Zn5), especially Zn5, are important for the heterochromatin localization of Sall1 protein.

Sall family proteins have conserved amino acid sequences in the recognition helix, and these sequences are important for localization to heterochromatin

Next, we produced GFP-fusion proteins of all the other Sall family members, and introduced them into NIH3T3 cells. Sall1 and Sall3 have five zinc finger clusters (ten zinc fingers in total), while Sall2 and Sall4 have four clusters (eight fingers in total). Interestingly, Sall4 showed a similar localization pattern to Sall1 (Fig. 3A). Although a chick Sall3 homolog, csal-3, was reported to be localized in the cytoplasm (Sweetman *et al.* 2003), mouse Sall3 was localized in both the cytoplasm and the nucleus. Sall3 in the nucleus was localized to heterochromatin in a similar pattern to Sall1 and Sall4. Sall2 was localized in the nucleus, but showed a quite different pattern from

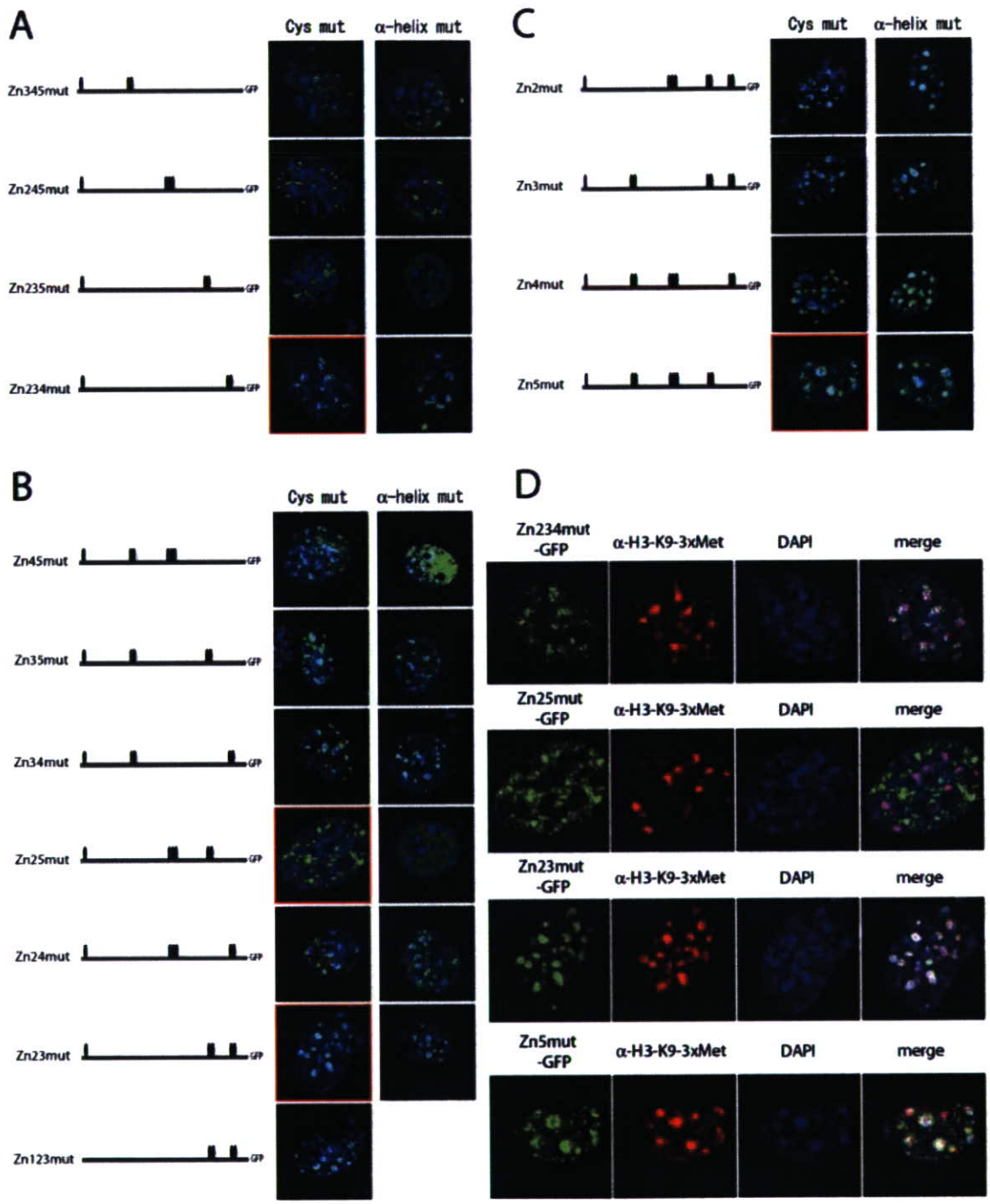

Figure 2 Localization of Sall1 to heterochromatin requires the C-terminal double zinc fingers Zn4 and Zn5. (A) Diagrams and localizations of GFP-fused Sall1 mutants that have one intact double zinc finger in addition to the most N-terminal C2HC zinc finger. (B) Diagrams and localizations of GFP-fused Sall1 mutants that have two intact double zinc fingers in addition to the most N-terminal C2HC zinc finger. (C) Diagrams and localizations of GFP-fused Sall1 mutants that have one impaired double zinc finger cluster. Left images: localizations of zinc finger cysteine mutants (cys mut); right images: localizations of recognition helix mutants (α-helix mut). Heterochromatin is indicated by DAPI staining (blue). The red boxes emphasize the importance of Zn4 or Zn5 for heterochromatin localization. (D) Localizations of the representative GFP-fused Sall1 cysteine mutants shown in the red boxes in (A–C). Heterochromatin is stained with an anti-tri-methylated H3K9 antibody (red) or DAPI (blue).

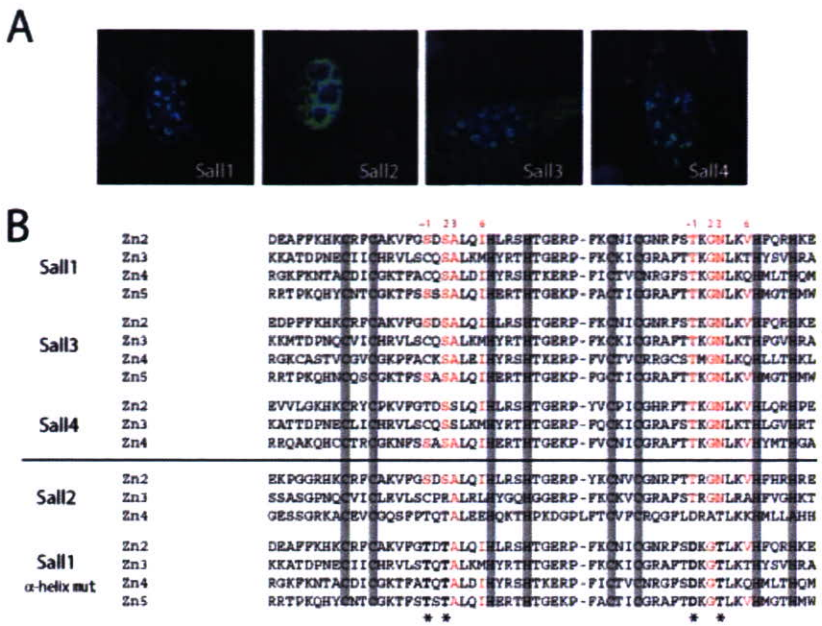

Figure 3 The amino acid sequences of the recognition α-helix are important for the localization to heterochromatin. (A) Localizations of four Sall family proteins fused to GFP. (B) Alignment of the amino acid sequences of all the double zinc finger domains from the four members of the Sall family, in addition to that of the Sall1 α-helix mutant. The red numbers indicate conserved amino acids at positions −1, 2, 3 and 6 in the recognition α-helix of the C2H2 zinc fingers. The most C-terminal zinc fingers are highly conserved among Sall1, Sall3 and Sall4, but not Sall2. Asterisks indicate amino acids replaced in Sall1 α-helix mut, mimicking the Zn4 domain of Sall2.

the other Sall family members, since it diffused uniformly throughout the nuclear compartments except for the DAPI-positive spots (Fig. 3A). To examine whether these localization differences were due to the sequences of the zinc finger motifs, we aligned the amino acid sequences of all the C2H2 double zinc finger domains among the four Sall family proteins (Fig. 3B). C2H2 zinc finger motifs are comprised of a β-strand and an α-helix. The α-helix (referred to as the recognition helix) contacts bases in the major groove of DNA, and four amino acids at positions −1, 2, 3 and 6 in the recognition α-helix were reported to define the four nucleotides recognized by C2H2 zinc finger domains (Pabo *et al.* 2001). The amino acids at these positions in Sall1, Sall3 and Sall4 are highly conserved, and in particular, the most C-terminal zinc fingers (Zn5 of Sall1 and Sall3, Zn4 of Sall4) have the same amino acid residues at these positions. In contrast, the corresponding amino acids in Zn4 of Sall2 are quite different from those of the other family members (Fig. 3B). Therefore, the heterochromatin localization of other Sall family members may be dependent on the sequence of the recognition α-helix of their most C-terminal double zinc finger. To confirm this hypothesis in Sall1, we changed the amino acid residues in the recognition α-helix of each of the zinc finger clusters of Sall1 to those of Sall2 Zn4 (α-helix mut; Fig. 3B, asterisks). As expected, the localization of the α-helix mutants showed similar patterns to the equivalent cysteine residue mutants (Fig. 2, α-helix mut). Considering the proposed role of the α-helix in the binding to DNA, our results suggest that at least in Sall1, the double zinc finger motifs may recognize some specific nucleotide sequences that could exist in heterochromatin.

Binding sequences in the C-terminal double zinc fingers of Sall1

To investigate whether the zinc fingers of Sall1 recognize specific nucleotide sequences, we performed the cyclic amplification and selection of targets (CASTing) technique as a binding site selection assay (Wright *et al.* 1991). For this assay, we used a bacterially-expressed truncate of Sall1 fused with glutathione-S-transferase (GST) (GST-Zn5; Fig. 4A). This truncate contained Zn5, which was identified as the most important zinc finger for heterochromatin localization (Fig. 2). The fusion protein was bound to glutathione-Sepharose beads (Fig. 4B) and then mixed with randomized double-stranded (ds) oligonucleotides. The dsDNA pulled down by GST-Zn5 was subjected to PCR amplification. After four cycles of the selection process, we carried out electrophoretic mobility shift assays (EMSAs) to examine the enhancement of the protein-DNA affinity. The dsDNA obtained after selection showed significantly higher affinity than the initial oligonucleotides (Fig. 4C), and no binding was detected when GST was used as a negative control. When the dsDNA was cloned into a vector and sequenced, A/T-rich sequences were obtained (Fig. 5A). From an alignment of these sequences, we propose the putative consensus sequences ATAA(A/T)(A/T) (Fig. 5B).

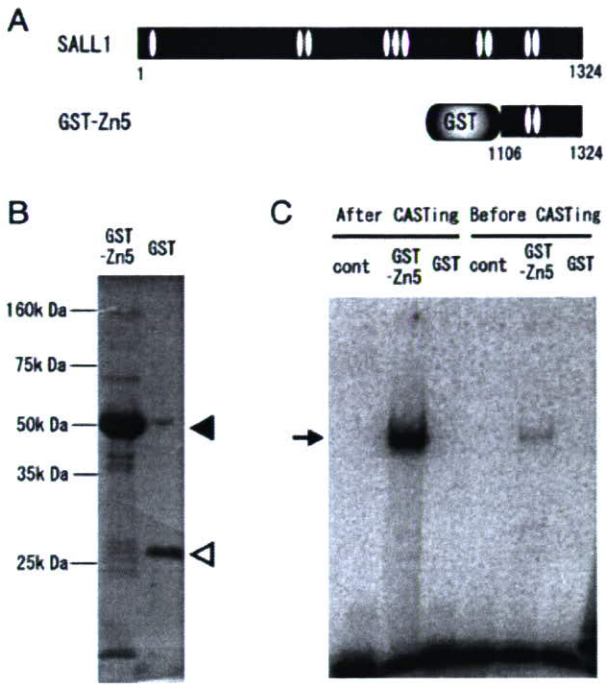

Figure 4 Generation of a GST-fused Sall1 deletion protein for CASTing. (A) Diagram of the GST-fused C-terminus of Sall1 (GST-Zn5). (B) Expression of GST-Zn5 is confirmed by SDS-PAGE and Coomassie Brilliant Blue staining (closed arrowhead). The open arrowhead indicates GST alone. (C) EMSAs reveal high-affinity binding of GST-Zn5 to the selected DNA after CASTing (arrow). EMSAs for GST protein and no protein (cont) were performed as negative controls.

To check whether these sequences have affinities for GST-Zn5, we performed EMSAs using four sequences (probes 1, 2, 3 and 4; Fig. 5A,C) or two oligonucleotides derived from probe 4 with point mutations (4-1 and 4-2; Fig. 5C,D) as probes. Probe 1, containing ATAAGA in its central portion, showed a weak interaction with Zn5-GST, while probes 2, 3 and 4, containing ATAATT or ATAAAA, showed clear band shifts. Probes 4-1 and 4-2, containing point mutations to the expected consensus sequence of probe 4, exhibited almost no binding to GST-Zn5. Thus the core consensus sequences of Sall1 Zn5 are likely to be ATAA(A/T)(A/T). These A/T-rich consensus sequences are consistent with the Sall1 localization to heterochromatin, since pericentric heterochromatin is mainly composed of major satellite DNA, which contains repetitive 234 bp A/T-rich sequences (Fig. 6A).

Sall1 binds to major satellite DNA

To determine whether Sall1 associates with major satellite DNA, we performed EMSAs using nuclear extracts from HEK293 cells expressing Sall1. Sall1 bound strongly to major satellite DNA as a clear band, indicating that a Sall1-DNA complex was formed. In contrast, a control nuclear extract (mock) with GFP expression showed no complex formation (Fig. 6B, lanes 1, 2). To examine which region of the major satellite DNA Sall1 associates with, we divided the major satellite DNA into three fragments, designated as Major A, B and C (Fig. 6A). Sall1 associated with all three fragments, but the strongest interaction was observed with Major B (Fig. 6B, lanes 3–8). The band for the Sall1-DNA complex was supershifted upon addition of an anti-Sall1 antibody (α-Sall1), and disappeared after the addition of excess cold major satellite DNA (Fig. 6C, lanes 1–5). These observations indicate that Sall1 specifically associates with major satellite DNA. To confirm this association, we performed EMSAs using nuclear extracts containing several zinc finger mutants. Zn23mut showing heterochromatin localization (Fig. 2B) associated with both full-length major satellite DNA (data not shown) and the Major B fragment, while Zn2-5mut and Zn45mut showing diffuse distributions in the nucleus (Fig. 2B) did not (Fig. 6C, lanes 6–8). These findings indicate that Sall1 binds to major satellite DNA via its C-terminal double zinc fingers.

Sall1 recognizes A/T-rich sequences present in major satellite DNA

Since Sall1 had a higher affinity for the Major B fragment than the other two fragments (Fig. 6B), we produced four deletion probes deleted from the 5′- or 3′-end of the Major B probe (B-1, B-2, B-3 and B-4; Fig. 7A), and performed EMSAs using these deletion probes. The deletion probes B-2, B-3 and B-4, which contained multiple A/T-rich sequences similar to the Zn5 consensus sequences, had stronger affinities for Sall1 than probe B-1, which contained one copy of the A/T-rich sequence (Fig. 7B).

To determine whether Sall1 did indeed recognize the consensus-like A/T-rich sequences, we produced another mutant probe, B-3mt, in which the T nucleotides of the A/T-rich sequences were replaced with C. As expected, Sall1 showed only weak association with this mutant probe (Fig. 7C, lanes 1–6). Furthermore, addition of an excess amount of cold B-3 fragments, but not B-3mt, interfered with binding of the B-3 probe to Sall1 (Fig. 7C, lanes 7, 8). Therefore, Sall1 could bind to the A/T-rich sequences that exist in major satellite DNA. Since these A/T-rich sequences are similar to the consensus sequences detected by the CASTing method, Sall1 may bind to the major satellite DNA of heterochromatin directly, thereby localizing itself to heterochromatin.

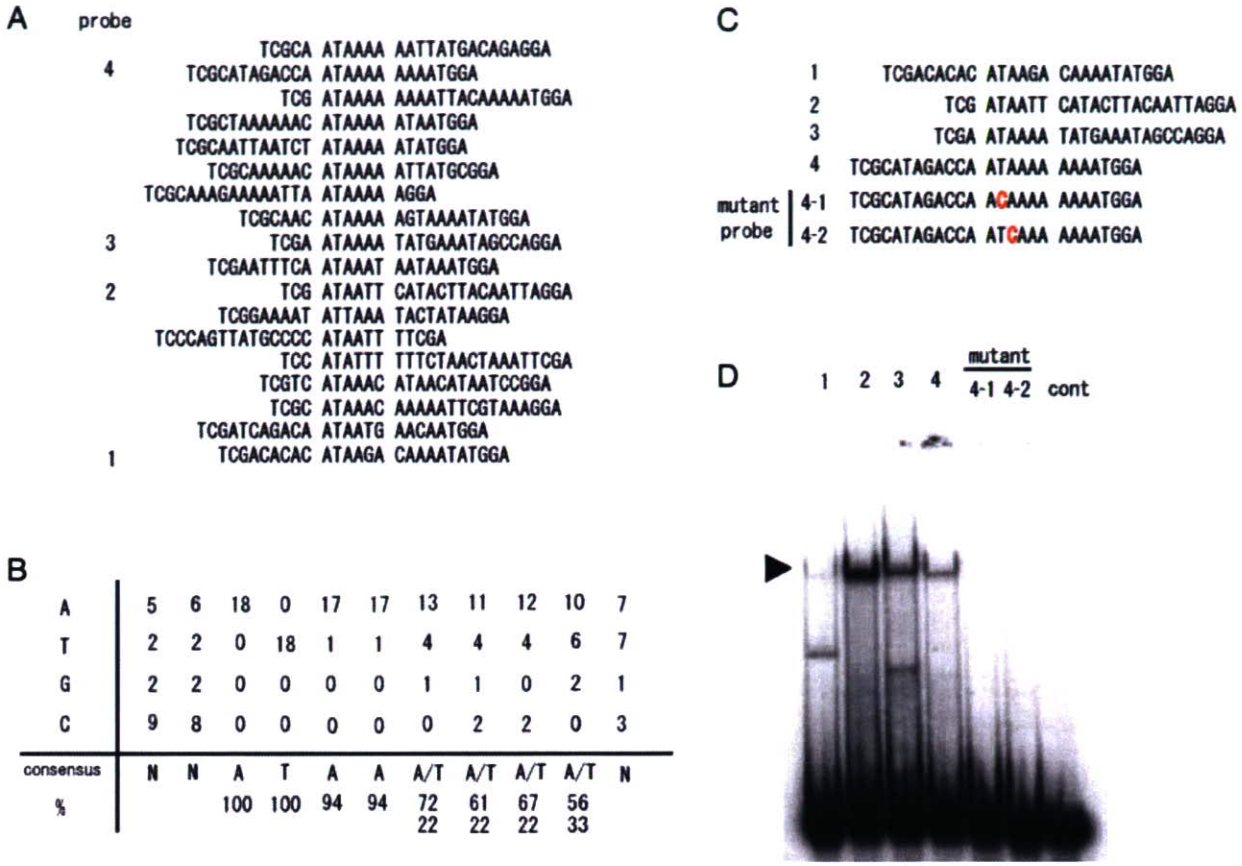

Figure 5 Characterization of the nucleotide sequences recognized by the GST-Zn5 fusion protein. (A) Aligned sequences of 18 clones obtained by CASTing. Probes 1, 2, 3 and 4 are identical to those in Fig. 5C. (B) Number and frequency of the nucleotides at each position. (C) Sequences of probes 1, 2, 3 and 4 and mutant probes 4-1 and 4-2. (D) EMSAs confirming the affinities between GST-Zn5 and the probes shown in (C). Probe 4 with no protein was also assayed as a negative control.

Discussion

Sall family proteins play important roles in a variety of organs, and most of the members are localized to heterochromatin. Here, we have shown that Sall1 is localized to heterochromatin via its C-terminal zinc fingers and that the most C-terminal double zinc finger (Zn5) has a high affinity for A/T-rich DNA sequences. Furthermore, Sall1 binds strongly to A/T-rich sequences of the major satellite DNA in heterochromatin. Thus, we have revealed the mechanism of the heterochromatin localization of Sall1, namely binding of the C-terminal zinc fingers of Sall1 to the major satellite DNA in heterochromatin. Zinc fingers typically function as interaction modules and bind to a wide variety of compounds, such as nucleic acids, proteins and small molecules (Pabo *et al.* 2001). Although it is possible that Sall1 binds to heterochromatin indirectly through interactions with other heterochromatin components, our data favor direct binding to the DNA, since Zn5 contains specific DNA-binding sequences and mutations in its recognition helix impair the localization. These findings are reminiscent of *Drosophila Salr*, which also binds to A/T-rich sequences, although its endogenous binding targets are unknown (Barrio *et al.* 1996).

Mutations in Townes–Brocks syndrome are often found in the region between Zn1 and Zn2 of Sall1 (Kohlhase 2000). In addition, mice expressing C-terminally-truncated Sall1 mimic the symptoms of Townes–Brocks syndrome, while *Sall1*-null mice do not. These data may be explained by a dominant-negative effect of the truncated Sall1 protein. Since the C-terminal zinc fingers are responsible for the heterochromatin localization, the C-terminally truncated Sall1 protein could be mislocalized from heterochromatin and may bind to other Sall family proteins through its N-terminal

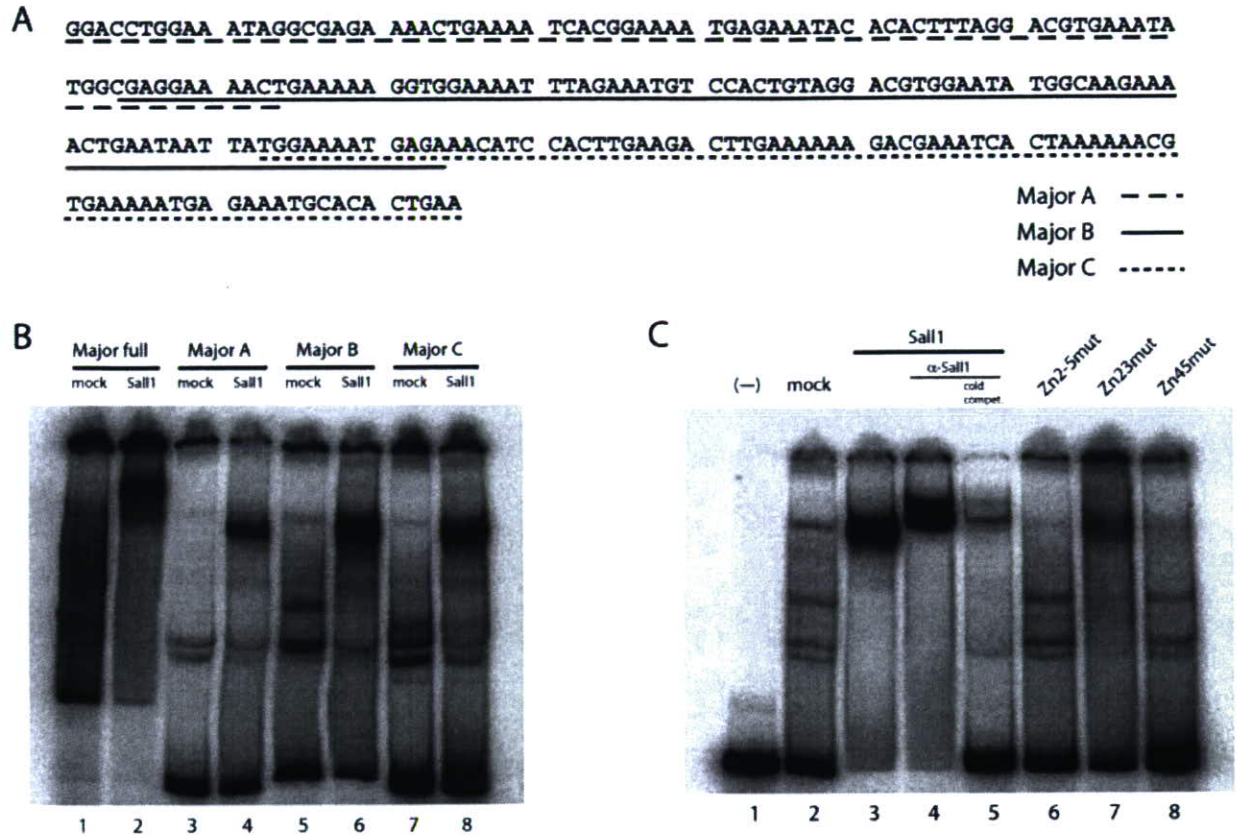

Figure 6 Sall1 binds to major satellite DNA. (A) Major satellite DNA sequences used for EMSAs. The bars indicate the Major A, Major B and Major C fragments, respectively. (B) EMSAs showing the binding of Sall1 to the full-length major satellite DNA, as well as the Major A, Major B and Major C fragments. Mock indicates a nuclear extract from HEK293 cells transfected with pCAGEN-EGFP as a control. (C) EMSAs using the Major B probe. Full-length Sall1 was used in lanes 1–5, and zinc finger mutants were used in lanes 6–8. A supershift assay (lane 4) and cold competition assay (lane 5) were also performed.

dimerization domain, as reported previously (Kiefer *et al.* 2003; Sweetman *et al.* 2003). Since Sall2 is not localized to heterochromatin and *Sall2*-deficient mice show no obvious abnormalities (Sato *et al.* 2003), mislocalization of Sall3 and Sall4 may be responsible for Townes–Brocks syndrome-like phenotypes in mice. Indeed, we recently showed that mice heterozygous for both *Sall1* and *Sall4* exhibit some of these abnormalities and that Sall1 and Sall4 form heterodimers (Sakaki-Yumoto *et al.* 2006). Since truncated Sall1 caused mislocalization of Sall4 from the heterochromatin, some of the Townes–Brocks syndrome-like phenotypes may result from Sall4 inhibition by truncated Sall1, functioning in a dominant-negative manner.

If this holds true in humans, the onset mechanisms of Townes–Brocks syndrome may be explained by mislocalization of SALL family members to non-heterochromatic regions via truncated SALL1. However, species differences in the pathogenesis of the disease should be taken into account. Some patients with deletion of the whole *SALL1* gene on one allele still exhibit the disease (Borozdin *et al.* 2006). Thus *SALL1* haploinsufficiency in humans can cause a mild Townes–Brocks syndrome phenotype, while Sall1 heterozygous mice show no unusual phenotypes. However, the reported phenotype is milder than that of the classical mutations, suggesting that truncated SALL1 resulting from the classical mutations may inhibit other SALL family members, thereby leading to more severe phenotypes. Regardless of the initial genetic event, the phenotypes should be caused by impairment of SALL functions, and humans may simply be more sensitive to dosage reduction of SALL1 than mice. Therefore, it remains an open question whether SALL functions are relevant to its localization to heterochromatin.

Although we have revealed the mechanism of the heterochromatin localization of Sall1, the functions of Sall1 at this nuclear region still remain unknown. Sall1 may be

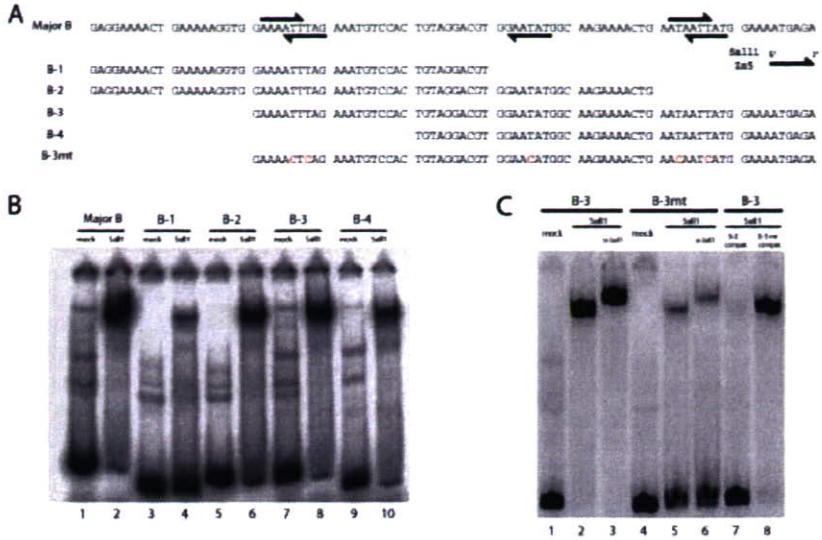

Figure 7 Sall1 recognizes the AT-rich sequences of major satellite DNA. (A) Major B deletion and mutant probes. The arrows indicate A/T-rich sequences similar to the Sall1 Zn5 consensus sequences (5′→3′). The positions of the point mutations are shown in red. (B) EMSAs using Major B deletion mutants. (C) EMSAs showing the affinity attenuation for B-3mt (lanes 1–6). Excess amounts of non-labeled B-3 and B-3mt were added to show the binding specificity (lanes 7 and 8, respectively).

involved in the formation or maintenance of heterochromatin. Sall1 was reported to associate with HDAC and several components of the NuRD chromatin remodeling complex (MTA1, MTA2 and RbAp46/48) (Kiefer *et al.* 2002; Lauberth & Rauchman 2006). By binding to the major satellite DNA and recruiting these remodeling factors to heterochromatin, Sall1 could participate in the formation or maintenance of chemical modifications of histones or DNA in heterochromatin. Alternatively, Sall1 may function as a transcriptional regulator similar to Ikaros, another C2H2 zinc finger protein that also localizes to heterochromatin and associates with major satellite DNA. Sall1, as well as Ikaros, may regulate gene expression by repositioning target gene loci to heterochromatin (Brown *et al.* 1997; Cobb *et al.* 2000; Koipally *et al.* 2002). To test this hypothesis, it is necessary to identify the direct downstream targets and demonstrate the association of these loci with Sall1. Recently, it was reported that Sall4, in cooperation with Tbx5, up-regulates *Fgf10* in developing forelimbs and both up-regulates *Gja5* and down-regulates *Nppa* in the developing heart (Koshiba-Takeuchi *et al.* 2006). In zebrafish, *sall1a*, the ortholog of *Sall1*, functions with *sall4* and regulates *fgfr2* and *fgf10* expressions in pectoral fin development (Harvey & Logan 2006). Thus it is necessary to test whether the gene loci of *Fgf10* and other potential Sall1 targets in mammals are associated with heterochromatin. Finally, Sall1 may bind to A/T-rich sequences in the promoter region of target genes that do not associate with heterochromatin. Although our data suggest that this is less likely, it remains possible that a small amount of Sall1 protein exists in non-heterochromatic regions and regulates gene expression as a transcription factor. In any case, it is necessary to identify the direct target genes of Sall1 and the molecules it associates with. Taken together, our data have revealed the heterochromatin localization mechanism of Sall1, and further elucidation of Sall1 functions at this site would lead to better understanding of organ development and the mechanisms of Townes–Brocks syndrome.

Experimental procedures

Plasmids

A Sall1-GFP expression vector (pCAGEN-Sall1-GFP) and N-terminal HA-tagged Sall1 expression vector (pCAGEN-HA-Sall1) were produced as described previously (Sato *et al.* 2004) from pCAGEN, a mammalian expression vector driven by the CAG promoter (Niwa *et al.* 1991). Sall1 zinc finger mutants were produced by replacing each of the zinc finger clusters of pCAGEN-Sall1-GFP with mutated fragments. Site-directed mutagenesis was performed by PCR using a Sall1 cDNA as a template and primers designed to alter the cysteine residues of each zinc finger to glycine, producing Zn1-5mut. In α-helix Zn2-5 mut, α-helix amino acids were changed to the Sall2 form. All PCR reactions were carried out using *Pfu* DNA polymerase (Promega). Each zinc finger mutant fragment amplified by PCR was cloned into pCR-Blunt II-TOPO (Invitrogen) and verified by sequencing. The Zn1 point mutant fragment was excised by *EcoRI* digestion, the Zn2 mutant by *SacI* and *ApaI* digestion, the Zn3 mutant by *ApaI* and *XhoI* digestion, the Zn4 mutant by *XhoI* and *SpeI* digestion and the Zn5 mutant by *SpeI* and *AgeI* digestion, followed by in-frame replacement of wild-type Sall1 with each mutant fragment. pCAGEN-HA-tagged Zn2-5mut, Zn23mut and Zn45mut without GFP, which were used for EMSAs, were generated by replacing the *EcoRI-SfiI* fragment of pCAGEN-HA-Sall1 with fragments of pCAGEN-Zn2-5mut-GFP, pCAGEN-Zn23mut-GFP and pCAGEN-Zn45mut-GFP, respectively.